https://doi.org/10.5194/egusphere-2026-4584
Preprint. Discussion started: 14 August 2026

Antarctic meltwater induces competing climate feedbacks in an Earth system model coupled to an Antarctic ice melt emulator

Eveline C. van der Linden[1], Klaus Wyser[2], Erwin Lambert[1], André Jüling[1], Dewi Le Bars[1], Sybren Drijfhout[1,3], and Irene Trombini[4,5]

[1]Royal Netherlands Meteorological Institute, Utrechtseweg 297, 3731 GA, De Bilt, The Netherlands
[2]Rossby Centre, Swedish Meteorological and Hydrological Institute (SMHI), 601 76 Norrköping, Sweden
[3]Institute for Marine and Atmospheric Research Utrecht, Department of Physics, Utrecht University, Princetonplein 5, 3584 CC, Utrecht, The Netherlands
[4]Department of Physics and Astronomy, University of Bologna, Bologna, Italy
[5]Institute for Atmospheric Sciences and Climate, National Research Council of Italy, Bologna, Italy

Correspondence: Eveline C. van der Linden (linden@knmi.nl)

Abstract. Antarctic ice-sheet mass loss is expected to accelerate under future warming, yet its climatic impacts remain poorly represented in Earth system models. Here, we present simulations with the EC-Earth3 Earth system model that incorporate the Antarctic Ice Melt Emulator (AIME), interactively coupled to the ocean component. AIME simulates regionally and temporally varying freshwater fluxes driven by subsurface ocean temperatures over the Antarctic continental shelf, accounts for the delayed dynamic response of the ice sheet, and enables two-way interactions between the climate system and Antarctic ice loss.

Under an abrupt quadrupling of atmospheric CO_2, the interactive freshwater forcing gives rise to two distinct feedback regimes. During the transient adjustment phase, enhanced freshwater input strengthens Southern Ocean stratification, suppresses vertical mixing, and modifies continental shelf circulation, leading to enhanced subsurface warming near the base of Antarctic ice shelves. During the subsequent quasi-equilibrium phase, the dominant climatic response shifts: reduced surface warming, increased sea-ice persistence, and decreased global ocean heat uptake weaken the atmospheric warming, ultimately reducing subsurface warming over the Antarctic continental shelf despite continued freshwater input.

Compared with a simulation without interactive Antarctic freshwater forcing, the coupled simulation exhibits lower equilibrium climate sensitivity and reduced global ocean heat storage under identical greenhouse-gas forcing. These results demonstrate that Antarctic freshwater feedbacks evolve over time, with an initial ocean-driven amplification followed by a longer-term atmosphere-mediated damping response. Our findings highlight the importance of representing interactive Antarctic freshwater fluxes in Earth system models to capture coupled ice-sheet-ocean-atmosphere feedbacks and improve projections of future climate change.

1 Introduction

The Antarctic Ice Sheet (AIS) and the Southern Ocean are tightly coupled through a range of feedback mechanisms that play a critical role in regulating Antarctic contributions to global sea-level rise, ocean circulation, and climate (Fyke et al., 2018; Holland et al., 2020; Mackie et al., 2020b; Li, 2022; Sadai et al., 2025). Despite their importance, these feedbacks remain

https://doi.org/10.5194/egusphere-2026-4584
Preprint. Discussion started: 14 August 2026

poorly constrained and are a major source of uncertainty in long-term sea-level projections (Siahaan et al., 2022; Park et al., 2023). A central element of this coupling is the impact of freshwater (FW) discharge from Antarctic ice-sheet mass loss on the stratification and thermal structure of the Southern Ocean (Gorte et al., 2023). These fluxes are expected to intensify under anthropogenic climate forcing and strongly influence temperatures over the Antarctic continental shelf, with important implications for ice-ocean interactions (Thomas et al., 2023).

The observed sea level contribution of Antarctica is currently largely driven by interactions with the ocean through melting underneath floating ice shelves (Pritchard et al., 2012; Rignot et al., 2019). The ice shelves play an important role in buttressing the grounded ice (Gudmundsson, 2013). When these ice shelves thin or collapse due to ocean-driven melting, the flow of grounded ice into the ocean can accelerate, leading to increased discharge and subsequent sea level rise by adding mass to the ocean (Rignot et al., 2019). Recent projections indicate that continued ocean warming could lead to widespread thinning or loss of Antarctic ice shelves over the coming centuries, with profound implications for ice-sheet stability and future ice mass loss (Hill et al., 2024; Burgard et al., 2025). Although the mass loss of floating ice shelves does not directly contribute to sea level rise, the total FW flux from the AIS to the ocean due to basal melting includes contributions from floating ice and grounded ice (Paolo et al., 2015).

Freshwater forcing experiments have been instrumental in advancing understanding of the Southern Ocean response to Antarctic meltwater input (Pauling et al., 2016; Park and Latif, 2019; Swart et al., 2023). These idealized simulations apply prescribed FW fluxes to isolate the impacts of meltwater discharge on ocean circulation, stratification, and heat distribution. Across studies, surface freshening is found to enhance stratification, suppress vertical mixing, and promote subsurface heat accumulation (Pauling et al., 2016; Bronselaer et al., 2018; Golledge et al., 2019). This subsurface warming can substantially increase basal melt rates, particularly in regions where warm Circumpolar Deep Water accesses the continental shelf (Jenkins et al., 2010), giving rise to a positive feedback in which enhanced basal melting strengthens FW input and further amplifies subsurface warming.

However, recent multi-model analyses indicate that meltwater-driven feedbacks for subsurface ocean warming exhibit strong regional variability in magnitude and even sign under future warming scenarios (Muilwijk et al., 2025). Moreover, the sea-ice response to FW forcing is not consistent across models: while many studies report increases in sea-ice extent following Antarctic meltwater input (Bintanja et al., 2013; Pauling et al., 2016, 2026), others find little or no such response (Swart and Fyfe, 2013). Beyond the Southern Ocean, coupled climate model experiments show that increasing Antarctic meltwater discharge can induce large-scale circulation adjustments and surface cooling, with implications for global climate sensitivity (Bronselaer et al., 2018; Purich and England, 2023; Sadai et al., 2020; Mistry et al., 2025). The anomalous atmospheric cooling constitutes a negative feedback on Antarctic ice mass loss that counteracts the positive subsurface warming feedback, highlighting the competing processes that govern ice-ocean-climate interactions (Park et al., 2023; Li et al., 2024).

The climatic impact of Antarctic meltwater depends not only on its volume but also on its spatial and vertical distribution in the ocean (Moon et al., 2025; Basinski-Ferris et al., 2025). Although FW released near the surface tends to reduce sea surface salinity and intensify stratification, leading to cooling of sea surface temperatures and warmer subsurface temperatures, in reality the distribution is more complex. Observations indicate that about half of the melt occurs at depth underneath the

https://doi.org/10.5194/egusphere-2026-4584
Preprint. Discussion started: 14 August 2026

ice shelves (Rignot et al., 2013). In contrast to surface injection, meltwater discharged at depth can generate a cooling effect on subsurface ocean temperatures in some regions (Thomas et al., 2023). Incorporating a more realistic representation of Antarctic meltwater has been shown to improve the simulation of observed Southern Ocean climate trends in Earth system models (ESMs; Rye et al., 2020), highlighting the importance of accurately representing meltwater inputs in ESMs.

Despite growing evidence for the importance of meltwater-driven feedbacks, global climate models participating in the Coupled Model Intercomparison Project Phase 6 (CMIP6) represent Antarctic FW fluxes in a highly simplified manner. In many models, FW fluxes from Antarctic mass loss are based on excess snowfall, without taking into account interactions between ice sheet processes and ocean circulation (Nowicki et al., 2016). Consequently, CMIP6-class models misrepresent the effects of meltwater on ocean stratification and subsurface warming and the associated feedbacks that can accelerate or decelerate ice sheet retreat (Holland et al., 2020). Only a small number of climate models currently include a dynamically coupled Antarctic Ice Sheet component, enabling two-way ice-ocean-atmosphere feedbacks, including the CMIP6-class UKESM (Smith et al., 2021; Siahaan et al., 2022) and AWI-ESM (Gierz et al., 2020) and the intermediate complexity model LOVECLIP (e.g., Park et al., 2023). However, studies of ice sheet-ocean feedbacks using coupled ESM-ice sheet models are mainly constrained by unrealistic simulations of the Antarctic ocean (Beadling et al., 2020; Smith et al., 2021), rather than by limitations of the coupling approach itself.

The potentially important role of meltwater-driven feedbacks in regulating Antarctic Ice Sheet (AIS) mass loss highlights the need for improved coupling between the AIS and the Southern Ocean in climate models. Although fully coupled ice-sheet-climate models provide a physically consistent framework for simulating these interactions, their availability remains limited and their application is constrained by climate model biases. Consequently, the sensitivity of Antarctic ice loss to oceanic forcing and associated feedbacks is not captured in current ice mass loss projections.

To address this gap, we have developed the Antarctic Ice Melt Emulator (AIME), which simulates ocean-driven AIS mass loss and is interactively coupled to the ocean component of the ESM EC-Earth3 (Döscher et al., 2022). In AIME, the magnitude of ocean-driven AIS mass loss is computed using linear response functions derived from a dynamic ice-sheet model, representing the delayed total ice-mass response to enhanced basal melt anomalies. AIME thus provides a complementary approach to fully coupled ice-sheet-climate models, enabling efficient exploration of large-scale ice-ocean-climate feedbacks while remaining grounded in process-based model behavior. Here, we use AIME to assess how meltwater-driven feedbacks linking Antarctic ice loss to ocean thermal structure may influence AIS mass loss and global climate change.

Our analysis spans regional to global scales. We first quantify the Antarctic freshwater forcing and its effects on subsurface ocean temperatures over the continental shelf. We then investigate the regional mechanisms underlying the climate response, including upper-ocean freshening, stratification, vertical mixing, changes in the Antarctic Slope Current and Circumpolar Deep Water supply, sea-ice evolution, and surface heat fluxes. Finally, we examine the large-scale oceanic and atmospheric responses, including changes in the global energy balance, to assess how these processes feed back on Antarctic subsurface temperatures and meltwater release. Together, these analyses reveal two distinct freshwater-driven feedback regimes: an initial amplification of subsurface shelf warming driven by oceanic processes, followed by a longer-term damping response associated with large-scale atmospheric adjustment.

https://doi.org/10.5194/egusphere-2026-4584
Preprint. Discussion started: 14 August 2026

2 Models and experimental design

2.1 EC-Earth3

Model simulations were conducted using the standard configuration of EC-Earth3 (Döscher et al., 2022). The ocean model is Nucleus for European Modelling of the Ocean (NEMO) version 3.6 and contains 75 vertical levels, including the Louvain-la-Neuve Ice Model (LIM3) for simulating sea ice. The atmosphere is represented by the Integrated Forecast System (IFS) cycle 36r4 of the European Centre for Medium-Range Weather Forecasts (ECMWF), including the land surface module HTESSEL, and contains 91 vertical layers. The model was set up with the ORCA1 grid (nominally 1° grid resolution) for the ocean and sea ice components and a T255 (ca. 80 km) grid for the atmosphere and land components.

The standard EC-Earth3 configuration does not include a land ice component. Antarctica is represented by a fixed 10 m water-equivalent perennial snow layer, of which only 1 m is thermodynamically active. Snow can accumulate, but summer temperatures are insufficient to remove the excess, which would lead to an unrealistically increasing snowpack. To prevent this, a snow excess removal scheme is applied that removes snow exceeding the 10 m threshold and routes it to the ocean, where it is melted and treated as calving. This provides a highly simplified representation of real ice-sheet dynamics, in which ice flow transports accumulated mass to the ocean, where it is released through iceberg calving and basal melting of ice shelves. The resulting FW input to NEMO is added as ice and therefore extracts latent heat from the ocean during melting, unlike runoff, which only adds mass.

2.2 The Antarctic Ice Melt Emulator

In this study, Antarctic ice-sheet FW fluxes are computed interactively using the Antarctic Ice Melt Emulator (AIME), which replaces the Antarctic "ice sheet" in EC-Earth3 (Sect. 2.1) and introduces a feedback between subsurface ocean temperatures over the Antarctic continental shelf and meltwater release. As a result, Antarctic meltwater fluxes are driven by oceanic rather than atmospheric changes and are interactively affecting the FW fluxes of the ocean model. Changes in liquid runoff from surface melt are not included in the anomalous FW fluxes. The following sections describe how the magnitude and temporal evolution of Antarctic FW release are diagnosed from ice-sheet linear response functions (Sect. 2.2.1), and how this FW is partitioned, spatially distributed, and thermodynamically treated in the ocean model (Sect. 2.2.2).

2.2.1 Freshwater forcing magnitude

AIME computes Antarctic FW release using ice-mass linear response functions (LRFs) derived from ice-sheet model experiments forced by basal melt anomalies. The LRFs are obtained from the LARMIP-2 basal melt perturbation experiments of Levermann et al. (2020), which consist of 200-year simulations with a constant anomalous basal melt of 8 m/yr. While Levermann et al. (2020) provide LRFs for sea-level rise, a substantial fraction of Antarctic mass loss – primarily from ice shelves and grounded ice below sea level – does not contribute to sea-level change but still represents a FW flux that can affect ocean circulation and climate feedbacks. We therefore use ice-mass loss LRFs (Fig. 2a) rather than sea-level LRFs, as described in

https://doi.org/10.5194/egusphere-2026-4584
Preprint. Discussion started: 14 August 2026

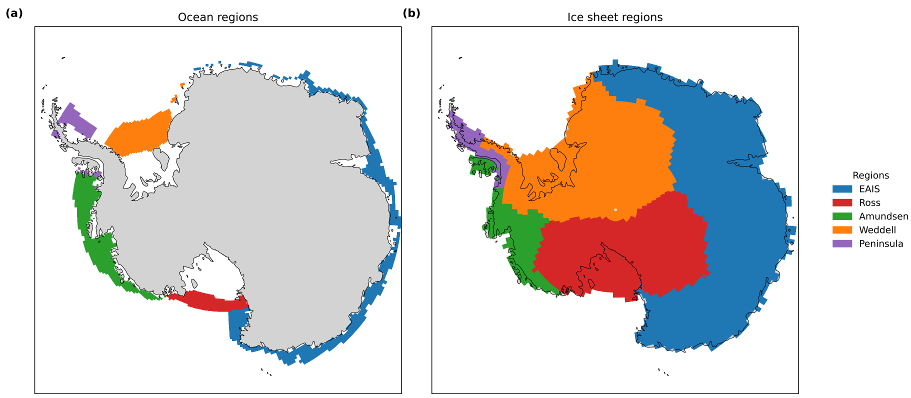

Figure 1. (a) Ocean and (b) ice sheet regions in AIME. The ocean sectors are based on LARMIP-2 (Levermann et al., 2020), with a fifth additional region for the Antarctic Peninsula similar to van der Linden et al. (2023). Different from the aforementioned studies ocean sectors only include grid cells over the continental shelf (south of the 1000 m isobath). The ice sheet regions are similar to LARMIP-2.

Lambert et al. (2025). These LRFs link basal melt beneath ice shelves to the delayed total FW release from the Antarctic ice sheet, including both sub-shelf melt and iceberg melt, and have units of Gt/m. By construction, they capture the long-term ice-sheet response up to 200 years, extending well beyond the initial ocean forcing perturbation.

In AIME, the Antarctic ice sheet is divided into five regions, being Ross, Amundsen Sea Embayment, Antarctic Peninsula, Weddell, and East Antarctic Ice Sheet (EAIS), each forced by annual-mean subsurface ocean temperatures from the corresponding ocean sector (Fig. 1a,b). For each region, ice mass loss is computed using an LRF derived from a dynamic ice-sheet model, which describes the 200-yr response to a 1 m/yr basal melt perturbation. Basal melt forcing is diagnosed from the subsurface ocean temperatures averaged between 200 and 700 m depth, representative of a typical ice-shelf draft. A quadratic basal melt parameterisation is applied in each region to relate ocean thermal forcing to anomalous basal melt (van der Linden et al., 2023). The resulting basal melt anomalies are then used to force the regional LRFs and compute total FW release.

Regional quadratic melt sensitivities are derived from simulations with the LADDIE basal melt model (Lambert et al., 2023). Mean basal melt rates are evaluated for each ice shelf under four idealized thermal forcing scenarios (present-day, +0.5, +1, and +2,°C; Lambert and Burgard, 2025), accounting for vertical temperature structure and local bathymetry. Regional mean melt rates and thermal forcing are computed as area-weighted averages across ice shelves, with an additional (0,0) point included to anchor the relationship at zero forcing. A quadratic function is fitted to these data, and the resulting coefficient defines the regional quadratic melt sensitivities used in AIME (Table 1).

For this study, we use LRFs from the fast Elementary Thermomechanical Ice Sheet model (f.ETISh; Pattyn, 2017), which yields total ice mass loss consistent with the ISMIP6 'MeanAnt' scenario (Seroussi et al., 2020) in a standalone setup forced by EC-Earth3 (Fig. 2b). Total FW release is estimated by assuming a constant regional fraction of basal melt relative to total ice mass loss, following the observations of Rignot et al. (2013). The same regional fractions are used in Lambert et al. (2025). Compared to an idealized fit to ISMIP6 'MeanAnt' (Swart et al., 2023), AIME shows an earlier acceleration of ice mass loss. It

https://doi.org/10.5194/egusphere-2026-4584
Preprint. Discussion started: 14 August 2026

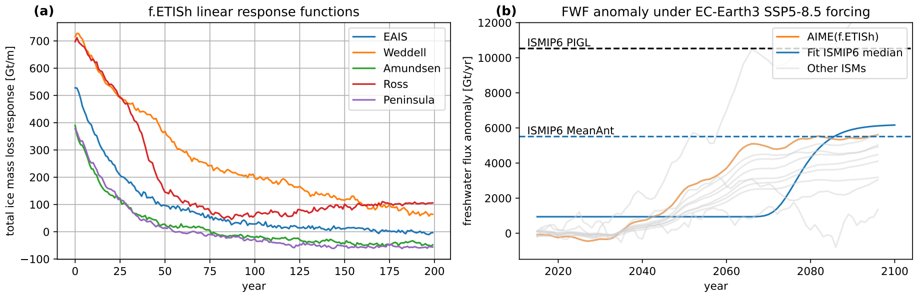

Figure 2. (a) Total ice mass loss linear response functions (LRFs) for the f.ETISh ice sheet model for the five regions in Figure 1b. (b) FW flux anomaly simulated by AIME over 2015-2100 under historical (to simulate the delayed response to basal melting) and SSP5-8.5 forcing from EC-Earth3 (standalone) with LRFs of 10 different ice sheet models (ISMs; grey lines), including the f.ETISH ISM used in the the current study (orange line). The lines are smoothed with a 10-yr running mean filter. The two dashed lines illustrate estimates of the magnitude of total ice mass loss anomalies by 2100 from ISMIP6 'MeanAnt' and 'PIGL' experiments (Seroussi et al., 2020) The blue line illustrates an idealised fit for the ISMIP6 'MeanAnt' total ice mass loss projections from (Swart et al., 2023).

should be noted that, although the LRFs peak immediately following a step perturbation, this does not imply an equally rapid increase in FW release. Instead, FW release results from the convolution of the LRF with continuously evolving basal melt anomalies, so the response reflects the integrated effect of past forcing. As basal melt anomalies increase gradually under the SSP5-8.5 forcing, the freshwater response remains relatively constant during the first decades before increasing more rapidly.

In the climate model, the anomalous FW fluxes are computed as the year-to-year difference in the cumulative FW flux. This anomaly is added to a climatological mean FW flux derived from precipitation minus evapotranspiration over Antarctica during a baseline period at the start of the experiment (Fig. 3a).

2.2.2 Geographical distribution and latent heat

The FW flux anomaly provided to EC-Earth3 is partitioned into two components representing basal melting of ice shelves and melting of calved icebergs, allowing for the representation of their differing impacts on the climate system (Mackie et al., 2020a). Total freshwater release is estimated by assuming region-specific basal-melt fractions relative to total ice mass loss, following the observational estimates of Rignot et al. (2013), with the remainder attributed to calving. While these fractions are fixed for each region, the Antarctic-wide contribution of basal melt to total freshwater release varies over time because the relative importance of individual regions changes. The resulting basal-melt and calving freshwater fluxes are prescribed with distinct vertical and geographical distributions, representing the local release of freshwater at depth and the offshore transport and surface melting of icebergs, respectively.

Because EC-Earth3 does not explicitly represent ice-shelf cavities, basal meltwater is inserted in ocean grid cells directly in front of the Antarctic coastline (Fig. 3b) over the depth range of the ice-shelf base as a proxy for sub-shelf melt, using a vertical distribution similar to that adopted by Mathiot et al. (2017). Accordingly, the FW is applied between 200 and 700 m depth, where 200 m represents the typical calving-front depth and 700 m approximates the grounding-line depth, or the local seabed

https://doi.org/10.5194/egusphere-2026-4584
Preprint. Discussion started: 14 August 2026

Table 1. Basal melt sensitivities for each ocean sector, derived from LADDIE (Lambert and Burgard, 2025).

Region	Sensitivity (m yr^{-1} K^{-2})
East Antarctic	1.19
Ross	0.33
Amundsen	0.43
Weddell	0.96
Peninsula	0.18

where it is shallower. Within this depth interval, ocean temperature is reduced to account for the latent heat of fusion required to melt the ice, and temperature and salinity are adjusted to represent the mixing of the added FW with seawater.

The calving component is applied at the ocean surface and distributed over a broader region surrounding the Antarctic continent (Fig. 3c), representing the drift and melt of icebergs away from the coast. The associated FW flux is imposed as ice in the surface ocean grid cells and therefore extracts latent heat from the ocean during melting.

The geographical distributions of basal melt and iceberg melt are prescribed using the basal-melt and calving masks from Lambert et al. (2025), which are consistent with the five Antarctic ocean sectors used to force AIME (Fig. 1a). For basal melting, the mask is extended by one ocean grid cell along the Antarctic coastline to ensure numerical continuity. Basal melt FW is inserted locally within the ocean sector associated with the corresponding ice-sheet region, reflecting the local character of sub-shelf melting. Iceberg transport is represented implicitly by distributing the calving-related FW flux across ocean sectors according to observed patterns of iceberg melt (Lambert et al., 2025). Within each sector, the calving FW flux is distributed uniformly by area, while the basal melt flux is distributed uniformly by volume.

2.3 Experiments

The baseline climate is taken from the EC-Earth3 piControl experiment, representing pre-industrial conditions (circa 1850) in its CMIP6 configuration, hereafter referred to as CTL (Table 2). To assess the impact of Antarctic ice-melt feedbacks, we compare an experiment with interactive FW flux anomalies computed by AIME (AIME-ON) to a standard EC-Earth3 experiment without AIME (NO-AIME). Both experiments are initialized from CTL restart files for the CMIP6 ensemble member r8i1p1f1 and are integrated for 165 years under abrupt-4×CO_2 forcing, in which atmospheric CO_2 is instantaneously quadrupled and then held constant. We use an abrupt-4×CO_2 experiment as idealized forcing to amplify ice sheet-climate feedbacks, facilitating diagnosis of the strength and mechanisms of ice-climate interactions. Finally, to diagnose Antarctic ice melt under abrupt-4×CO_2 forcing in the absence of climate feedbacks from FW release, we perform a standalone AIME simulation (ONLY-AIME) forced with subsurface ocean temperatures from the NO-AIME experiment.

https://doi.org/10.5194/egusphere-2026-4584
Preprint. Discussion started: 14 August 2026

Table 2. Experiments

Name	Model setup	CO_2	Melt	Feedback
CTL	EC-Earth3	piControl	Excess snow	No
NO-AIME	EC-Earth3	abrupt-4$\times CO_2$	Excess snow	No
AIME-ON	EC-Earth3-AIME	abrupt-4$\times CO_2$	AIME	Yes
ONLY-AIME	AIME	abrupt-4$\times CO_2$	AIME	No

3 Results

3.1 Freshwater fluxes and ocean forcing

The spatial distribution of freshwater fluxes originating from the Antarctic ice sheet, averaged over the 30-yr period with the largest AIME-ON minus NO-AIME differences in FW forcing, is shown in Fig. 3, highlighting the regional pattern of the freshwater forcing differences between the two simulations. The AIME baseline consists of the mean excess snowfall from the CTL simulation, which is distributed over a broad circumpolar belt (Fig. 3a). The basal melt and calving fluxes computed by AIME are imposed as anomalies added to this baseline (Fig. 3b,c).

The total Antarctic ice-sheet freshwater flux in AIME-ON, comprising the baseline flux together with the basal-melt and calving anomalies generated by the interactive response to subsurface ocean temperatures (Fig. 3d), is compared with the equivalent Antarctic ice-sheet freshwater flux in NO-AIME, approximated by the excess snowfall anomaly, calculated as the integrated precipitation minus evaporation over the Antarctic continent (Fig. 3e). The resulting differences (Fig. 3f) highlight both an increase in the total freshwater input and a redistribution of freshwater. Relative to NO-AIME, AIME-ON introduces substantially more freshwater close to the Antarctic continent, whereas freshwater input is reduced farther offshore. In contrast, the Weddell Sea exhibits the largest positive offshore freshwater anomalies, reflecting enhanced iceberg melt associated with the calving component.

The time evolution of the Antarctic FW flux anomalies in AIME-ON is compared with the NO-AIME experiment in Fig. 4. Anomalies are defined relative to the CTL mean excess snowfall of 3315 Gt/yr in EC-Earth3, which serves as the baseline FW distribution in AIME-ON and represents an approximately 20% high bias relative to observational estimates (Depoorter et al., 2013). In AIME-ON, the FW flux anomaly increases rapidly, reaching a peak of approximately 10,000 Gt/yr after about 50 years, when global mean surface air temperature has risen by about 5.5 K and subsurface ocean temperatures over the continental shelf by about 1.7 K. Thereafter, the anomally gradually declines to around 5,000 Gt/yr over the following 50 years, despite an additional $\sim$1 K warming of subsurface waters. This decline is consistent with a progressive reduction in the availability of ice for melting as ice shelves thin or are lost, leading the coupled system towards a new quasi-equilibrium state. This peak-and-decline behavior is broadly consistent with recent multi-model projections of Antarctic mass loss, which show an initial acceleration in ice-shelf melt, with some models exhibiting a subsequent decline as ice shelves weaken or disappear

https://doi.org/10.5194/egusphere-2026-4584
Preprint. Discussion started: 14 August 2026

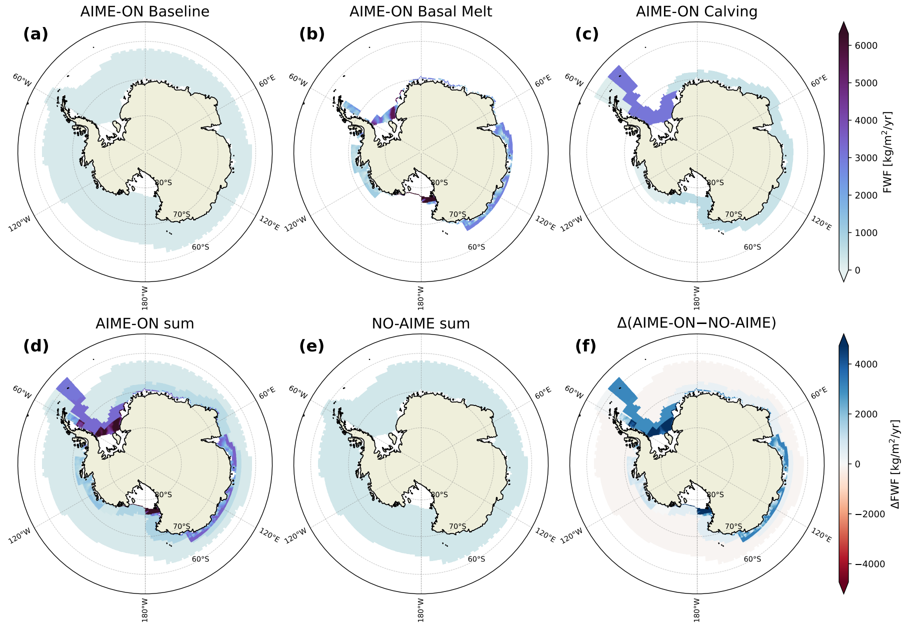

Figure 3. Freshwater flux distributions during Period A under abrupt-4×CO_2 forcing in EC-Earth3 coupled to the Antarctic Ice Melt Emulator (AIME-ON) and in the standard EC-Earth3 CMIP6 configuration (NO-AIME). Panels show (a) baseline freshwater flux, (b) basal meltwater flux, (c) calving freshwater flux, (d) total freshwater flux in AIME-ON, (e) total freshwater flux in NO-AIME, and (f) the difference in total freshwater flux (AIME-ON - NO-AIME).

(Seroussi et al., 2024). Relative to NO-AIME, the FW flux anomaly in AIME-ON is more than seven times larger at its peak and remains approximately three times larger after the subsequent decline.

To quantify the effect of interactive climate-ice-sheet coupling on Antarctic meltwater release, the AIME-ON simulation is compared with the standalone ONLY-AIME experiment (Fig. 4). In ONLY-AIME, basal melt is forced offline by prescribed subsurface ocean temperature anomalies and therefore captures the direct thermodynamic response of ice-shelf melt to ocean warming. Unlike AIME-ON, however, the resulting freshwater fluxes do not feed back onto the climate system through changes in ocean circulation and stratification. Differences between the two simulations therefore isolate the effect of two-way climate-ice-sheet coupling on Antarctic freshwater release.

During the first ∼70 years of the abrupt-4×CO_2 experiment, FW flux anomalies in AIME-ON are generally larger than in ONLY-AIME, indicating that climate-ice feedbacks enhance freshwater release during the initial response. Thereafter, the two simulations converge, and eventually AIME-ON exhibits smaller freshwater flux anomalies than ONLY-AIME, consistent with feedbacks that moderate melt over longer timescales.

Feedback strength (defined in Fig. 4) initially increases following a brief adjustment period, indicating positive climate-ice feedbacks that enhance Antarctic meltwater release. It subsequently declines and becomes negative, indicating a transition to feedbacks that reduce meltwater release relative to the uncoupled response. This behaviour reflects a two-timescale response

https://doi.org/10.5194/egusphere-2026-4584
Preprint. Discussion started: 14 August 2026

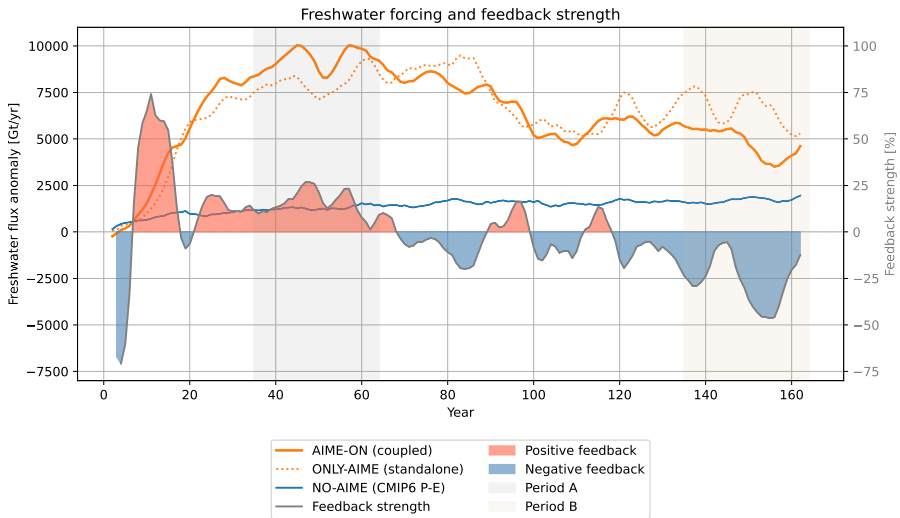

Figure 4. Freshwater flux anomalies under abrupt-4×CO_2 forcing. Shown are the Antarctic freshwater flux anomalies for AIME-ON (with feedbacks; orange solid line) and ONLY-AIME (without feedbacks; orange dotted line). Feedback strength is defined as the relative difference between the AIME-ON and ONLY-AIME freshwater flux anomalies, normalized by the ONLY-AIME anomaly and expressed as a percentage. The blue line shows the freshwater flux associated with Antarctic excess snowfall in NO-AIME. All time series are smoothed using a 5-year rolling mean.

to coupling: a fast, positive feedback that enhances Antarctic melt during the transient climate adjustment to abrupt-4×CO_2 forcing, followed by a slower, negative feedback that weakens the response as the system approaches a new quasi-equilibrium.

To examine these feedback regimes in more detail, we define two analysis periods: the transient feedback phase (Period A; model years 35-64) and the quasi-equilibrium feedback phase (Period B; model years 135-164). Although the relative feedback strength reaches its maximum earlier in the simulation, Period A is defined as the 30-year interval centred on the maximum additional freshwater flux (AIME-ON minus ONLY-AIME), as this represents the time when climate-ice coupling has the largest absolute impact on the freshwater forcing experienced by the ocean.

Averaged over Period A, the relative feedback strength is +15%, indicating that climate-ice coupling enhances Antarctic freshwater release by approximately 15% relative to the uncoupled response. During Period B, the relative feedback strength is -26%, indicating that coupling reduces freshwater release relative to the standalone response. Although FW fluxes also decline in ONLY-AIME, reflecting the delayed response of the ice sheet to ocean forcing, the reduction is substantially greater in AIME-ON, highlighting the damping effect of climate-ice feedbacks.

The basal melt driving the FW flux anomalies is computed from subsurface ocean temperatures averaged between 200 m and 700 m depth over the Antarctic continental shelf (south of the 1000 m isobath). The impact of coupling Antarctic meltwater release to subsurface ocean temperatures can therefore be assessed by comparing the AIME-ON and NO-AIME simulations.

https://doi.org/10.5194/egusphere-2026-4584
Preprint. Discussion started: 14 August 2026

In the first half of the abrupt-4×CO_2 experiment, subsurface ocean temperatures warm more rapidly in AIME-ON than in NO-AIME (Fig. 5). Around the midpoint of the simulation, as the climate approaches a new equilibrium state, subsurface temperatures in AIME-ON converge back toward those in NO-AIME and become cooler by the end of the experiment, despite the persistently larger FW input in AIME-ON (Fig. 4).

To assess the magnitude of these anomalies relative to internal variability, we compare the mean AIME-ON minus NO-AIME temperature differences during Period A (model years 35-64) and Period B (model years 135-164) with the standard deviation of the corresponding piControl variability. The mean anomaly during Period A is +0.163 °C, equivalent to 1.68σ, while the mean anomaly during Period B is -0.145 °C, equivalent to -1.49σ (Fig. 5). Both anomalies exceed one standard deviation of the simulated internal variability, indicating that the coupled freshwater feedback generates decadal subsurface temperature anomalies outside the typical ($\pm 1\sigma$) range of natural variability.

The subsurface ocean temperatures that drive the FW flux anomalies thus exhibit a time-dependent response to the coupling, characterized by relative warming during the transient adjustment phase (Period A) and relative cooling during the later quasi-equilibrium phase (Period B). In the following sections, we investigate the mechanisms responsible for this reversal, focusing on why subsurface shelf waters initially warm and subsequently cool in AIME-ON relative to NO-AIME, even though the FW fluxes remain substantially larger throughout the experiment.

3.2 Stratification and circulation changes over the Antarctic continental shelf

Changes in the magnitude and distribution of Antarctic ice melt strongly affect both vertical stratification and horizontal circulation over the continental shelf, with important consequences for shelf-open-ocean exchange. Figure 6 shows the evolution of temperature, salinity, squared buoyancy frequency, and zonal velocity anomalies averaged over the Antarctic continental shelf (south of the 1000 m isobath), together with the corresponding vertical profiles during Periods A and B. These diagnostics reveal how Antarctic meltwater modifies the vertical structure of the shelf ocean over time.

The additional freshwater generated by the coupled ice-sheet feedback produces a pronounced reduction in surface warming and enhanced freshening in AIME-ON relative to NO-AIME, while subsurface waters initially warm more strongly than in NO-AIME. This enhanced subsurface warming coincides with increased stratification, as indicated by the higher buoyancy frequency, which suppresses vertical mixing and reduces heat exchange between the surface and deeper layers. Consequently, more heat is retained at depth despite reduced surface warming during the transient feedback phase (Period A).

At the same time, zonal velocity anomalies reveal a strengthening of the westward-flowing Antarctic Slope Current (ASC) along the continental margin in AIME-ON relative to NO-AIME (Fig. 7), consistent with the idealized FW forcing experiments of Muilwijk et al. (2025). This intensification is associated with an enhanced cross-shelf density gradient, with fresher, lighter waters near the coast and saltier, denser waters offshore (Fig. A1), as explained by Ong et al. (2025). Through geostrophic (thermal wind) and hydrostatic balance, this enhanced density gradient increases vertical shear in the along-slope flow. However, the ASC is not purely geostrophic, and its net transport also depends on wind forcing, with regional variability along the continental slope (Thompson et al., 2018).

https://doi.org/10.5194/egusphere-2026-4584
Preprint. Discussion started: 14 August 2026

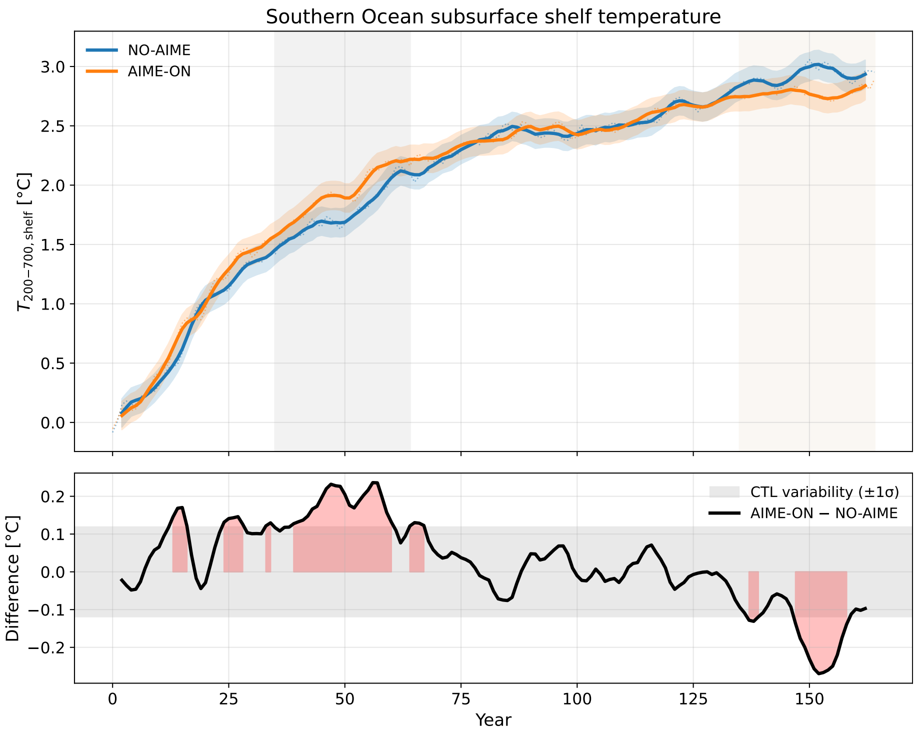

Figure 5. Time series of Southern Ocean subsurface shelf temperature in the NO-AIME and AIME-ON experiments. Shelf temperature is defined as the mean potential temperature averaged over the Antarctic continental shelf (south of the 1000 m isobath) between 200 and 700 m depth. Thin dotted lines show annual values, while thick solid lines show 5-year running means. Shaded envelopes around the solid lines indicate the $\pm 1\sigma$ range of 5-year mean shelf temperature estimated from the 500-year CTL simulation, representing the characteristic magnitude of internal variability. The lower panel shows the difference (AIME-ON - NO-AIME), with the grey band denoting the $\pm 1\sigma$ range of 5-year mean variability in the CTL simulation. Periods where the difference lies outside the grey band are highlighted in red, indicating that the AIME-induced response exceeds the typical magnitude of internal climate variability.

In principle, a strengthened ASC could act as a dynamic barrier that limits intrusions of relatively warm Circumpolar Deep Water (CDW) onto the continental shelf (Beadling et al., 2022). However, despite the intensified ASC, subsurface shelf waters are warmer in AIME-ON than in NO-AIME during Period A. This apparent contradiction can be understood in terms of the vertical structure of the current.The strengthening of the ASC is concentrated in the upper ocean, where stratification and horizontal density gradients are largest, while there are no clear differences in the strength of the current below the upper few hundred meters (Fig. 6d). This shoaling enhances baroclinic shear but reduces the deep-reaching component of the slope current, thereby weakening its effectiveness as a barrier at depth. Whether this change affects cross-shelf exchange and heat transport is investigated in later sections.

As the experiment progresses toward a new equilibrium (Period B), the freshwater anomaly over the continental shelf weakens. The reduction in freshwater forcing is accompanied by a gradual salinification of shelf waters relative to Period

https://doi.org/10.5194/egusphere-2026-4584
Preprint. Discussion started: 14 August 2026

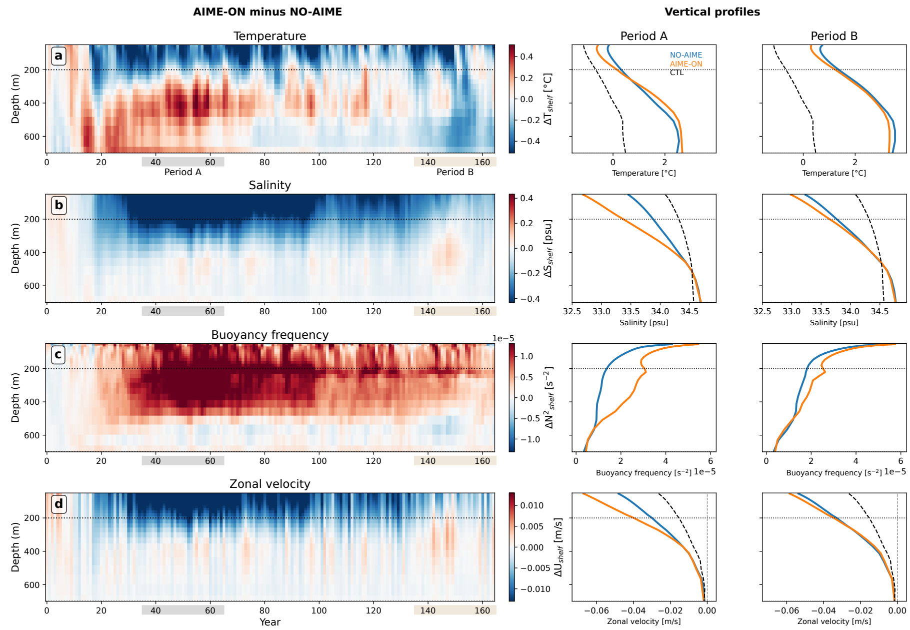

Figure 6. Evolution of Antarctic shelf-ocean properties under abrupt-4×CO_2 forcing. (a) Temperature (T), (b) salinity (S), (c) squared buoyancy frequency (N^2), and (d) zonal velocity (U), The left column shows Hovmöller diagrams of AIME-ON minus NO-AIME anomalies averaged over the Antarctic continental shelf south of the 1000 m isobath, illustrating the temporal evolution and vertical structure of the ocean response. Blue colours indicate lower values and red colours higher values relative to NO-AIME. The middle and right columns show the corresponding shelf-mean vertical profiles for Period A (model years 35–64) and Period B (135-164), respectively. NO-AIME is shown in blue, AIME-ON in orange, and the CTL simulation as a black dashed line. Dotted horizontal lines indicate depths of 200 m and 700 m, corresponding to the depth range used to compute the ocean forcing supplied to the Antarctic Ice Melt Emulator. Zonal velocity is defined as positive eastward. Negative zonal-velocity anomalies therefore indicate a strengthening of the westward Antarctic Slope Current relative to NO-AIME.

A, which weakens the cross-shelf density gradient and reduces the vertical shear and strength of the ASC in AIME-ON relative to its earlier state.

Although stratification remains stronger in AIME-ON than in NO-AIME throughout the experiment, this contrast diminishes over time as FW fluxes weaken. During Period B, subsurface shelf waters in AIME-ON become cooler relative to NO-AIME, indicating a shift in the dominant processes controlling shelf-ocean temperatures. Although stratification remains stronger in AIME-ON than in NO-AIME, its influence weakens as freshwater forcing declines. The emergence of relative subsurface cooling therefore suggests that processes other than local stratification become increasingly important in determining the shelf heat budget. The mechanisms responsible for this transition cannot be inferred from the temperature and zonal circulation changes alone and require an explicit analysis of the underlying heat fluxes.

https://doi.org/10.5194/egusphere-2026-4584
Preprint. Discussion started: 14 August 2026

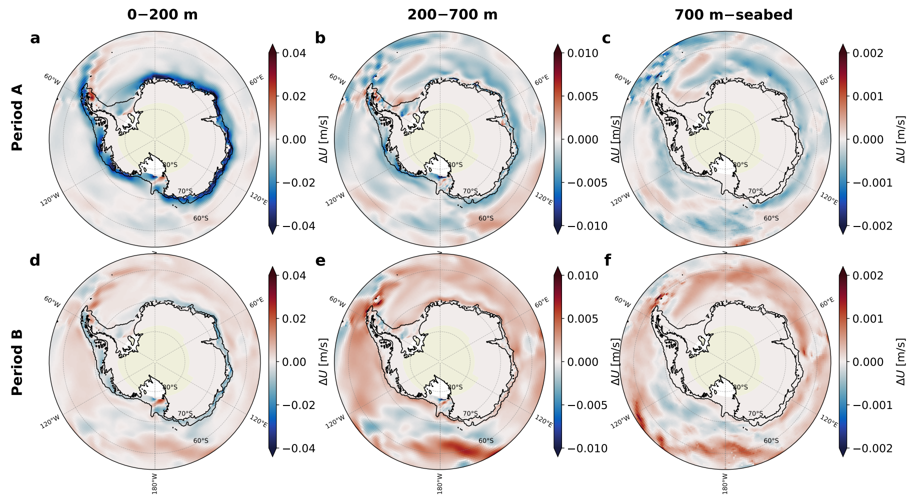

Figure 7. Depth-dependent zonal velocity anomalies under abrupt-4×CO_2 forcing. Shown are zonal velocity differences between the EC-Earth3 simulation coupled to the Antarctic Ice Melt Emulator (AIME-ON) and the EC-Earth3 CMIP6 configuration without interactive Antarctic meltwater feedbacks (NO-AIME), averaged over Period A (top row) and Period B (bottom row). Results are shown for three depth ranges: 0–200 m, 200–700 m, and 700 m to the seabed. Negative anomalies indicate a strengthening of the westward flow or a weakening of eastward flow relative to NO-AIME, whereas positive anomalies indicate a weakening of the westward flow or a strengthening of eastward flow. The black contour line marks the continental shelf break, defined by the 1000 m isobath. Note that colour scales differ between columns to highlight the spatial structure of the response.

This evolution highlights a time-dependent response of the coupled system: an early phase (Period A) characterized by enhanced stratification, a stronger surface-intensified ASC, and warmer subsurface shelf waters, followed by a later phase (Period B) with relative subsurface cooling despite continued freshwater anomalies and enhanced stratification. Understanding how these changes influence the shelf heat budget requires a more explicit examination of the underlying heat fluxes, which we investigate in the next section.

3.3 Surface-ocean response and sea-ice feedbacks

The additional Antarctic Ice Sheet (AIS) meltwater in AIME-ON produces a colder sea surface relative to NO-AIME under abrupt-4×CO_2 forcing. This relative cooling arises from the formation of a fresh, buoyant surface layer that enhances stratification and suppresses vertical mixing, thereby reducing the upward transport of heat from the subsurface ocean. The most pronounced surface cooling occurs over the Antarctic continental shelf, particularly in the Weddell Sea and the Amundsen-Bellingshausen sectors, where temperature anomalies locally approach –2 °C during Period A (Fig. A2). Surface cooling weakens during Period B but remains evident along much of the continental margin.

Sea-surface salinity exhibits a similar pattern, with widespread freshening over the Antarctic continental shelf and particularly strong anomalies in the Weddell Sea, where salinity decreases locally by up to about 0.75 psu during Period A (Fig. A1).

https://doi.org/10.5194/egusphere-2026-4584
Preprint. Discussion started: 14 August 2026

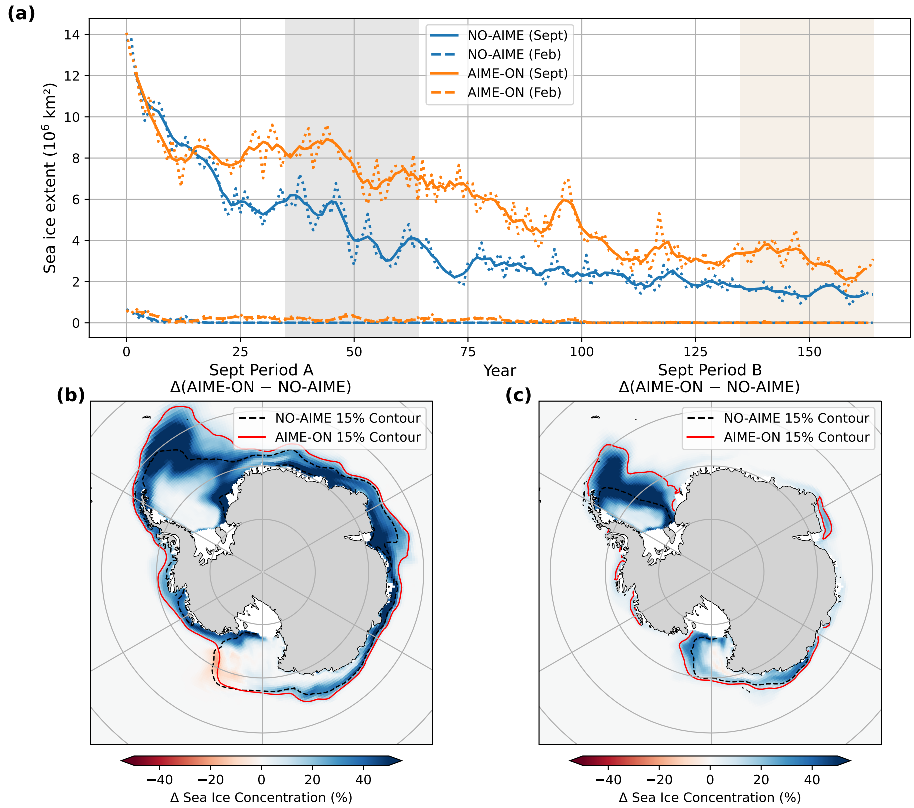

Figure 8. Southern Hemisphere sea ice under abrupt-4×CO_2 forcing. Panel (a) shows the time series of Southern Hemisphere sea ice extent at the annual maximum (September) and minimum (February), respectively, for the AIME-ON and NO-AIME simulations. Panels (b) and (c) show the differences in September sea ice concentration between AIME-ON and NO-AIME, averaged over Period A and Period B, respectively.

Freshening weakens during Period B but remains concentrated along the continental margin, whereas salinity anomalies over the open Southern Ocean are much smaller. This surface cooling and freshening suppress sea-ice loss in AIME-ON relative to NO-AIME, resulting in a larger Antarctic sea-ice extent throughout the experiment (Fig. 8).

Figure 8 shows the evolution of Antarctic sea-ice extent together with the September sea-ice concentration differences between AIME-ON and NO-AIME for Periods A and B. During the austral summer minimum (February), Antarctic sea ice remains nearly absent in both simulations throughout the experiment, consistent with the known low Antarctic sea-ice bias of EC-Earth3 (Döscher et al., 2022). In contrast, substantial differences emerge during the austral winter maximum (September). Antarctic sea-ice extent decreases rapidly during the first decades following abrupt-4×CO_2 forcing in both simulations, but remains consistently larger in AIME-ON than in NO-AIME throughout the experiment. The difference is greatest during Period A, when September sea-ice extent in AIME-ON exceeds that in NO-AIME by approximately 2-3 × 10^6 km^2, before gradually declining during the later stages of the simulation.

https://doi.org/10.5194/egusphere-2026-4584
Preprint. Discussion started: 14 August 2026

Spatially, the enhanced winter sea ice in AIME-ON is concentrated primarily in the Weddell Sea and along sectors of East Antarctica, where sea-ice concentration increases locally by more than 40% relative to NO-AIME during Period A (Fig. 8b). These regions coincide with the largest freshwater forcing, surface freshening, and surface cooling (Figs. 3, A2, and A1), consistent with the enhanced winter sea-ice extent. Smaller negative anomalies are also evident in parts of the Ross Sea. During Period B, the positive sea-ice anomalies weaken but remain most pronounced in the Weddell Sea. The 15% sea-ice concentration contour continues to extend farther north in AIME-ON than in NO-AIME over much of this region, consistent with the persistence of enhanced freshwater forcing and its associated surface freshening and cooling.

The persistence of surface cooling and enhanced sea ice suggests that Antarctic meltwater substantially modifies the exchange of heat between the ocean and atmosphere. To understand how these surface changes influence the development of the subsurface warming anomaly, we next examine the shelf-ocean heat budget.

3.4 Shelf-ocean heat budget

To understand how the subsurface warming anomaly develops, we examine the heat budget during the first 50 model years, which encompass the period of most rapid divergence in subsurface shelf temperatures between AIME-ON and NO-AIME (Fig. 5). The combined effect of all heat fluxes crossing the surface boundary of the liquid ocean is a pronounced spatial pattern (Fig. 9a), with reduced ocean heat loss (positive anomalies) over much of the Antarctic shelf and enhanced heat loss (negative anomalies) farther offshore.

Reduced sea-ice loss in AIME-ON increases the surface albedo relative to NO-AIME, causing a larger fraction of incoming solar radiation to be reflected back to space and thereby reducing surface warming (Fig. 9d). At the same time, the cooler and fresher surface layer, together with the greater sea-ice cover, suppresses upward turbulent heat fluxes to the atmosphere relative to NO-AIME (Fig. 9f), while cooler surface temperatures and enhanced sea ice also reduce upward longwave radiation (Fig. 9e). Together, these changes reduce heat loss from the ocean to the atmosphere, allowing more heat to be retained within the ocean.

Latent heat fluxes associated with iceberg melting also have a large influence on the surface ocean heat budget but act in opposition to the turbulent heat fluxes (Fig. 9b). Iceberg melting occurs at the surface and removes heat from the ocean, inducing additional surface cooling. In AIME-ON, this cooling is concentrated closer to the Antarctic coastline, whereas in NO-AIME iceberg melt occurs over a broader offshore region. As a result, iceberg melting contributes to relative surface cooling near the Antarctic coast and relative warming farther offshore in AIME-ON compared to NO-AIME. This spatial contrast is particularly evident in the Weddell Sea, where the iceberg melt pattern is clearly reflected in the net surface heat flux.

Taken together, these surface heat-flux changes indicate that the meltwater-induced surface freshening suppresses the upward transport of heat from the subsurface ocean, thereby reducing heat loss from from the ocean to the atmosphere and sea ice. During the first 50 years, the net heat loss from the ocean to the atmosphere, sea ice and icebergs over the Antarctic shelf is 49.6 TW in AIME-ON compared to 62.1 TW in NO-AIME, corresponding to a reduction of 12.5 TW (Fig. A3). This reduction persists throughout the simulation, averaging 14.6 TW during the next 100 years, indicating that the shelf ocean consistently loses less heat to the atmosphere, sea ice and icebergs in AIME-ON than in NO-AIME.

https://doi.org/10.5194/egusphere-2026-4584
Preprint. Discussion started: 14 August 2026

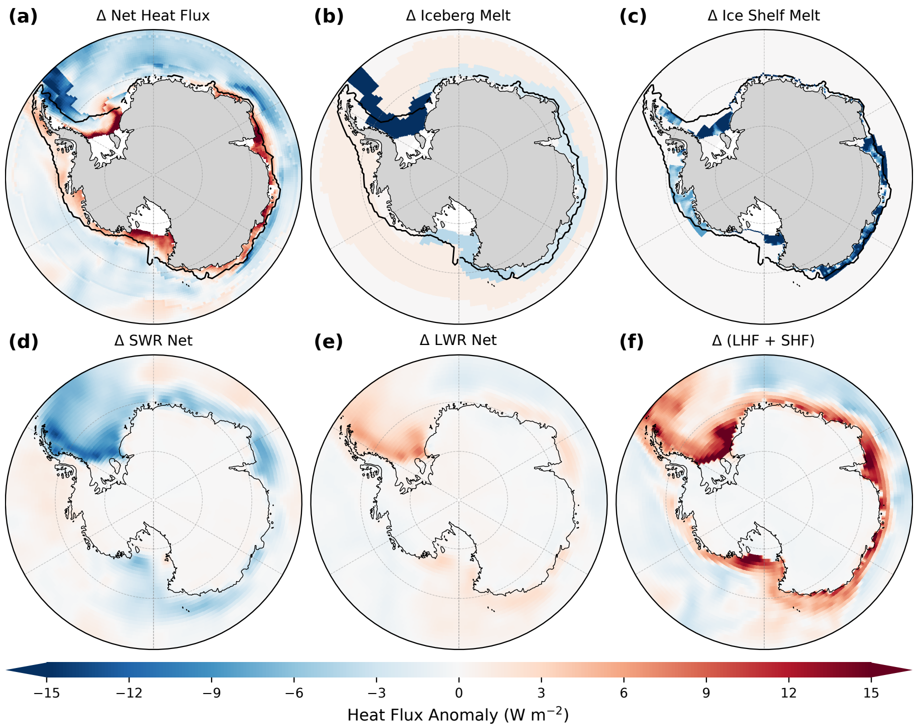

Figure 9. Differences in heat fluxes between AIME-ON and NO-AIME during the early adjustment period (model years 0-49). The top row shows heat fluxes entering the liquid ocean: (a) net downward heat flux at the sea surface, (b) latent heat consumed by iceberg melting at the sea surface, and (c) latent heat consumed by ice-shelf melting at depth (200-700 m). The black contour indicates the continental shelf break. The bottom row shows the atmospheric components of the surface energy budget over the ocean/sea-ice/land surface: (d) net downward shortwave radiation, (e) net downward longwave radiation, and (f) net turbulent heat flux (latent plus sensible heat; positive downward).

To close the heat budget of the Antarctic shelf, one must also consider basal melting. Basal melting of ice shelves represents an additional heat sink that is not included in the net surface heat flux. During the first 50 years, latent heat extraction associated with basal melting cools the shelf ocean by approximately 22.3 TW (Fig. A3). Because ice shelves melt at depth, this heat is extracted directly from subsurface waters, producing cooling between roughly 200 and 700 m depth (Fig. 9c). The basal-melt cooling exceeds the positive surface heat-flux anomaly, indicating that the diagnosed local surface and basal fluxes alone would produce a net cooling tendency.

During the first 50 years, the combination of enhanced subsurface heat storage and the imbalance between the positive surface heat-flux anomaly and the larger cooling associated with basal melting implies that local heat fluxes alone cannot account for the simulated temperature response. To close the heat budget, an additional positive ocean heat-transport convergence is therefore required in AIME-ON relative to NO-AIME. The residual ocean heat supply partly compensates for the cooling caused by basal melting and provides the additional heat required to sustain the enhanced subsurface warming. Also during the later stages of the simulation (years 50-100), neither the net positive surface heat-flux anomaly nor the cooling associated

https://doi.org/10.5194/egusphere-2026-4584
Preprint. Discussion started: 14 August 2026

with basal ice-shelf melting changes substantially relative to the first 50 years. The surface heat-flux anomaly remains smaller than the basal-melt cooling associated with the additional freshwater forcing. Neither of these local heat budget components can therefore explain the transition from enhanced subsurface warming to relative cooling. Although we do not diagnose ocean heat-transport convergence directly, the heat-budget analysis suggests that Antarctic meltwater forcing modifies the large-scale atmospheric and oceanic circulation in a manner that affects the delivery of ocean heat to the continental shelf.

3.5 Large-scale circulation changes and cross-shelf heat exchange

The heat-budget analysis suggests that changes in ocean heat transport, rather than local heat fluxes alone, are required to explain the evolution of the subsurface temperature anomalies. One possible mechanism is that Antarctic meltwater modifies the transport of ocean heat onto the continental shelf by altering the large-scale atmospheric and ocean circulation. In particular, changes in the winds, Antarctic Slope Current (ASC), Antarctic Circumpolar Current (ACC), and Southern Ocean overturning circulation (SOOC) may influence the delivery of relatively warm Circumpolar Deep Water (CDW) from the open Southern Ocean onto the shelf. We test this hypothesis by examining the response of these circulation components and assessing whether they are consistent with changes in cross-shelf heat transport.

The atmospheric circulation response differs markedly between the two periods (Fig. 10). During Period A, westerly winds strengthen over the midlatitudes near 40°S, while weakening occurs closer to Antarctica between approximately 55°S and 75°S. By Period B, the midlatitude strengthening weakens, whereas pronounced positive wind anomalies develop over high southern latitudes within the latitude band of the climatological Southern Ocean westerlies. This evolution is accompanied by enhanced cooling over Antarctica relative to lower southern latitudes, consistent with an increased meridional temperature gradient and stronger high-latitude westerlies.

The ocean circulation exhibits a broadly consistent evolution. During Period A, weaker high-latitude westerlies coincide with a stronger easterly Antarctic Slope Current (ASC) near the continental margin (Fig. 7), although the ASC response also reflects the enhanced coastal freshening and stratification discussed above. In Period B, stronger high-latitude westerlies are accompanied by a weaker ASC and a stronger Antarctic Circumpolar Current (ACC; Fig. A4), consistent with the expected ocean response to the wind changes. Taken together, these atmospheric and oceanic changes are consistent with the amplified high-latitude cooling strengthening the meridional temperature gradient and, in turn, contributing to the stronger ACC in AIME-ON relative to NO-AIME during the later stages of the experiment.

The SOOC also exhibits contrasting behaviour between the two periods. The large-scale upper overturning cell is weaker in Period A and stronger in Period B relative to NO-AIME (Fig. 11). This evolution is broadly consistent with the transition from weaker to stronger high-latitude westerlies, although the overturning response also depends on changes in surface buoyancy forcing. Freshwater input near Antarctica enhances upper-ocean stratification and influences dense-water formation, while sea-ice formation and melt further modify surface buoyancy. However, the reversal in SOOC anomalies between Periods A and B cannot be explained by freshwater forcing alone, since freshwater input remains larger in AIME-ON than in NO-AIME throughout the simulation. This indicates that the overturning response increasingly reflects the combined influence of wind forcing and buoyancy changes associated with sea-ice and dense-water formation, rather than freshwater forcing alone.

https://doi.org/10.5194/egusphere-2026-4584
Preprint. Discussion started: 14 August 2026

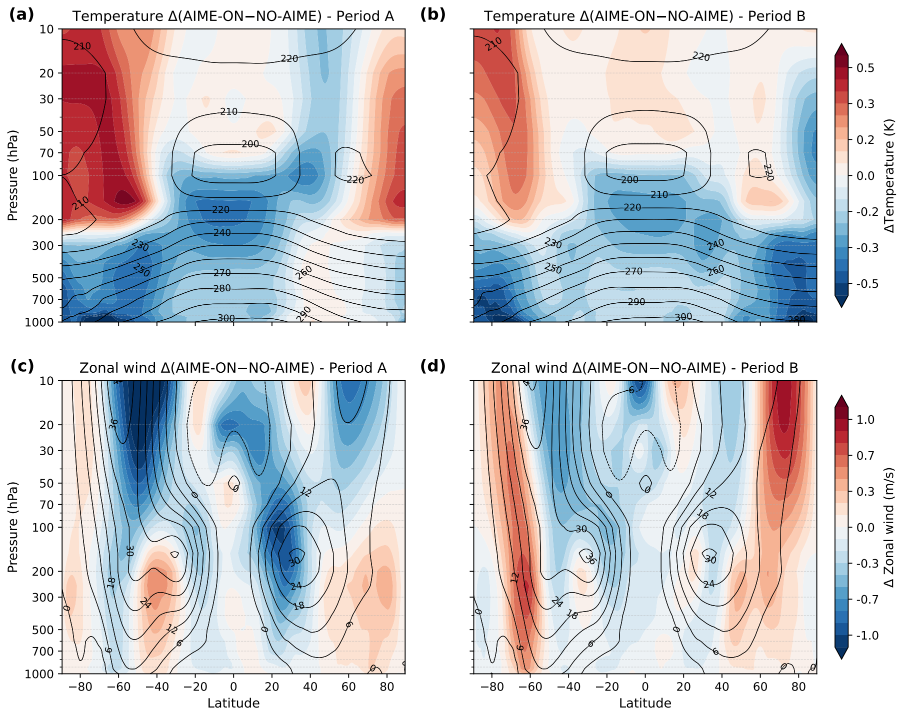

Figure 10. Vertical structure of atmospheric differences under abrupt-4×CO_2 forcing. Shown are zonal- and annual-mean differences in (a-b) air temperature and (c-d) zonal wind between AIME-ON and NO-AIME for Period A (left panels) and Period B (right panels). Black contours indicate the corresponding NO-AIME climatology for temperature and zonal wind, allowing the anomalies to be interpreted relative to the background atmospheric circulation.

In contrast to the large-scale upper overturning cell, over the continental shelf, the local clockwise overturning cell is strengthened in both periods, indicating an enhanced local overturning circulation (the freshwater pump). The freshwater pump is driven by the buoyant rise of basal meltwater, which induces a compensating inflow of deeper water toward the shelf. Such a circulation change could promote the on-shelf transport of relatively warm CDW, providing a plausible mechanism for enhanced heat delivery to the continental shelf.

A stronger upper SOOC is generally associated with enhanced upwelling of deep waters around Antarctica, while a stronger ACC and weaker ASC barrier would not be expected to inhibit exchanges between the open Southern Ocean and the continental shelf. In addition, the enhanced local shelf overturning (freshwater pump) could facilitate the transport of relatively warm Circumpolar Deep Water (CDW) onto the continental shelf. During Period A, the strengthened local shelf overturning provides a plausible mechanism for the enhanced ocean heat supply inferred from the heat-budget analysis, despite only modest changes in the large-scale circulation. During Period B, the stronger ACC, stronger upper SOOC, weaker ASC barrier, and enhanced local shelf overturning together provide a coherent dynamical framework for sustained or enhanced ocean heat supply to the Antarctic continental shelf. The freshwater forcing produces only a modest response in the Atlantic Meridional Overturning

https://doi.org/10.5194/egusphere-2026-4584
Preprint. Discussion started: 14 August 2026

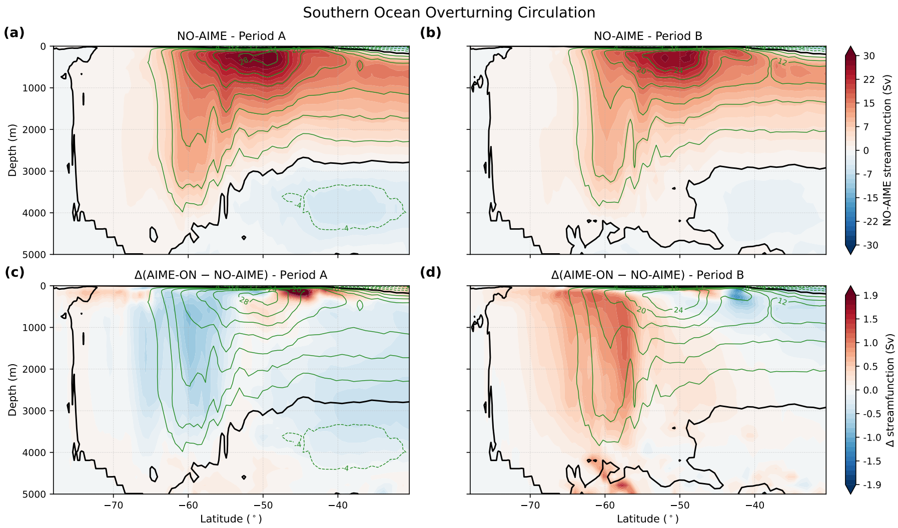

Figure 11. Southern Ocean meridional overturning circulation. The upper panels show the meridional overturning streamfunction in the NO-AIME simulation, averaged over 30-year periods for (a) Period A and (b) Period B. The lower panels show the corresponding differences between AIME-ON and NO-AIME. Green contours indicate the NO-AIME streamfunction, plotted at 4 Sv intervals; solid (dashed) contours denote positive (negative) values. Positive streamfunction values correspond to clockwise overturning, whereas negative values correspond to counterclockwise overturning. The overturning streamfunction is expressed as volume transport, obtained by converting from mass transport (kg s^{-1}) using a reference seawater density of 1027 kg m^{-3}.

Circulation (AMOC; Fig. A5), indicating that the simulated differences in climate response are not driven by major changes in Atlantic overturning.

While the available diagnostics do not permit a quantitative assessment of cross-shelf heat transport, they suggest that the transition from enhanced subsurface warming to relative cooling is controlled by broader changes in the climate system rather than by changes in large-scale ocean circulation. We therefore next examine whether differences in the global energy balance and climate sensitivity provide a more consistent explanation for the transition from enhanced subsurface warming to relative cooling.

3.6 Global energy balance and the reversal of the subsurface warming anomaly

The circulation analysis indicates that large-scale atmospheric and oceanic circulation changes do not provide evidence for a substantial reduction in ocean heat supply to the Antarctic continental shelf during Period B. At the same time, the heat-budget analysis showed that neither surface heat fluxes nor basal melting can explain the emergence of cooler subsurface shelf waters in Period B relative to Period A. We therefore consider a broader mechanism: changes in the global energy balance and climate sensitivity. If Antarctic meltwater feedbacks reduce the total amount of heat absorbed by the climate system, less heat will ultimately be available to warm the Southern Ocean and Antarctic shelf seas.

https://doi.org/10.5194/egusphere-2026-4584
Preprint. Discussion started: 14 August 2026

After the initial subsurface warming, subsurface ocean temperatures stabilize in both experiments as the climate system approaches a new equilibrium and the initial subsurface warming anomaly transitions to relatively cooler ocean temperatures by the end of the simulation (Period B). To assess whether this late-stage relative cooling is linked to changes in the global climate response, we first examine differences in equilibrium climate sensitivity (ECS).

ECS is defined as the increase in global mean surface air temperature (GSAT) following a doubling of atmospheric CO_2 relative to pre-industrial conditions, once radiative equilibrium is reached. Using the Gregory method applied to the abrupt-$4\times CO_2$ experiments, ECS is estimated to be 4.1 K for EC-Earth3-AIME and 4.3 K for EC-Earth3-CMIP6 (Fig. 12b) (Wyser et al., 2020; Zehrung et al., 2025). This difference indicates a modest reduction in the equilibrium warming response in the presence of interactive Antarctic FW forcing, despite identical imposed CO_2 concentrations.

In the early years of the abrupt-$4\times CO_2$ experiments, the top-of-atmosphere (TOA) energy imbalance is close to the effective radiative forcing of approximately 7 W m^{-2}. Most of this excess energy is initially absorbed by the ocean, resulting in a rapid increase in ocean heat storage, with a global ocean heat uptake rate of approximately 2.5×10^{15} W (Fig. 12a).

Adding FW around Antarctica freshens and stratifies the surface ocean, particularly in the Southern Ocean, and is associated with reduced ocean heat uptake and storage. Enhanced stratification suppresses vertical mixing and is consistent with reduced uptake of heat into the ocean interior, both locally in the Southern Ocean and more broadly through changes in the global overturning circulation, including a modest weakening of the AMOC (Fig. A5). As a result, global ocean heat uptake is reduced in AIME-ON relative to NO-AIME, especially during Period A when FW input is strongest (Fig. 4). Consequently, total ocean heat content remains lower throughout the simulation in AIME-ON (Fig. 12a). The persistent divergence in ocean heat content indicates that less heat is accumulated within the climate system when Antarctic meltwater feedbacks are included.

Over longer timescales, ocean heat uptake declines in both experiments as the system approaches equilibrium, decreasing to below 10^{15} W on multi-decadal timescales. Although the difference in ocean heat uptake between AIME-ON and NO-AIME becomes smaller by the end of the experiment, the cumulative ocean heat content remains lower in AIME-ON, indicating that less energy is stored in the ocean overall.

The reduced ocean heat uptake alters the atmospheric energy balance. Lower sea surface temperatures reduce heat and moisture exchange between the ocean and atmosphere, weakening the positive water vapour feedback, while reduced near-surface atmospheric warming strengthens the negative lapse-rate feedback. The persistence of greater sea-ice extent in AIME-ON further increases planetary albedo, limiting surface energy absorption and suppressing polar amplification. Together, these processes contribute to a lower equilibrium warming response in AIME-ON (Fig. 12b).

To link the reduced global warming to subsurface shelf temperatures, we examine the relationship between GSAT anomalies and ocean temperature anomalies over the Antarctic continental shelf between 200 and 700 m depth ($\Delta T_{200-700,\mathrm{shelf}}$; Fig. 12c). Subsurface shelf temperatures respond more slowly than GSAT, remaining nearly unchanged during the first stages of global warming before increasing approximately linearly once GSAT exceeds about 3-4 K. This delayed response reflects the slower adjustment of the Antarctic shelf ocean relative to the atmosphere following abrupt CO_2 forcing.

For a given level of global warming, subsurface shelf temperatures are higher in AIME-ON than in NO-AIME, consistent with the local effects of enhanced stratification and altered circulation discussed in previous sections. However, AIME-ON

https://doi.org/10.5194/egusphere-2026-4584
Preprint. Discussion started: 14 August 2026

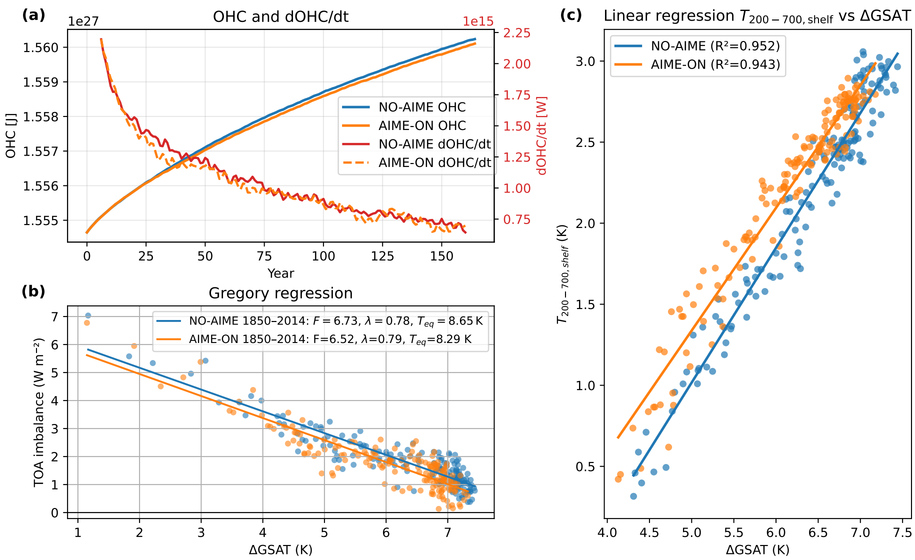

Figure 12. Ocean heat content and climate sensitivity diagnostics. (a) Time series of global ocean heat content (OHC), computed from ocean potential temperature using a constant reference density (ρ_0 = 1025 kg m^{-3}) and specific heat capacity (c_p = 3992 J kg^{-1} K^{-1}). Ocean heat storage is defined as the time derivative of OHC, calculated from annual means; a 10-year running mean is applied for smoothing. (b) Gregory plots showing the regression of global-mean top-of-atmosphere radiative flux anomalies (TOA imbalance) against global-mean surface air temperature anomalies (ΔGSAT). Anomalies are taken relative to the drift-corrected CTL simulation. (c) Linear regression between ΔGSAT and subsurface shelf temperature anomalies averaged over 200-700 m depth ($T_{200-700,\mathrm{shelf}}$), excluding the first 10 years of the simulation.

reaches a substantially lower equilibrium warming level because Antarctic meltwater feedbacks reduce ocean heat uptake and lower ECS. Consequently, the total amount of heat available to warm the Southern Ocean and Antarctic shelf seas is reduced. Although Antarctic meltwater feedbacks promote local subsurface heat retention through enhanced stratification and altered circulation, these regional effects operate within a climate system that accumulates less heat overall. By the end of the simulation, the reduction in global heat uptake outweighs the local tendency for enhanced subsurface warming, resulting in cooler Antarctic shelf waters in AIME-ON than in NO-AIME.

4 Discussion

Many previous freshwater-forcing studies have emphasized the positive feedback associated with meltwater-induced stratification, whereby reduced vertical mixing enhances subsurface warming and increases ice-shelf melt. Consistent with this mechanism, we find that Antarctic freshwater release initially promotes subsurface shelf warming and strengthens ice-sheet mass loss. However, this response is transient. As the climate system approaches equilibrium, reductions in ocean heat uptake, smaller reduction in sea-ice cover, and a weaker global warming response become increasingly important, eventually outweighing the local stratification feedback and leading to cooler subsurface shelf waters. These results suggest that assessments of

https://doi.org/10.5194/egusphere-2026-4584
Preprint. Discussion started: 14 August 2026

Antarctic meltwater feedbacks based solely on transient simulations may overestimate the long-term importance of the positive oceanic feedback.

More broadly, our results highlight the importance of distinguishing between local and global responses to Antarctic freshwater forcing. Locally, freshwater input modifies stratification, circulation, and the vertical distribution of ocean heat, creating conditions that favour enhanced ice-shelf melt. At the same time, freshwater forcing alters the global energy balance by reducing ocean heat uptake and moderating global warming. The long-term evolution of Antarctic shelf temperatures therefore reflects the competition between these regional oceanic processes and the global climate response. Understanding future Antarctic ice-sheet evolution thus requires consideration of both local Southern Ocean dynamics and their coupling to the wider climate system.

AIME provides a computationally efficient representation of Antarctic ice-sheet melt and freshwater release within a coupled climate-model framework. Compared with fully dynamic ice-sheet models, however, it necessarily relies on several simplifying assumptions. Antarctic ice melt is represented using linear response functions (LRFs), which assume that ice-sheet responses scale linearly with oceanic forcing. In addition, the LRFs are forced by anomalies in basal melt rather than absolute basal melt rates. This reduces the emulator's sensitivity to systematic biases in the simulated mean state of the Southern Ocean, which can strongly influence projections based on absolute thermal forcing. The linear formulation, however, does not capture nonlinear ice-sheet processes that may emerge under strong warming, such as marine ice-sheet or marine ice-cliff instabilities. Rather than replacing dynamic ice-sheet models, the LRF approach complements them by efficiently isolating climate feedbacks and facilitating systematic exploration of forcing-response relationships. In our experiments, the emulated basal melt responses are comparable in magnitude to those obtained in ISMIP6, suggesting that the emulator provides a physically plausible approximation of Antarctic melt sensitivity within its intended range of application.

The long-term evolution of freshwater forcing is also influenced by the delayed adjustment represented by the LRFs (Levermann et al., 2020). In the NO-AIME experiment, freshwater-flux anomalies scale approximately linearly with global mean surface air temperature because Antarctic surface mass balance responds directly to atmospheric warming (Fig. A6). Introducing AIME alters this relationship by adding a delayed ice-sheet response to subsurface ocean forcing. The LRFs are derived from dynamic ice-sheet simulations subjected to sustained basal-melt perturbations, in which meltwater fluxes decline as the ice-sheet system approaches a new equilibrium. This decline reflects the reduction in the area and volume of ice available for melting following substantial ice-shelf retreat, which outweighs the production of new floating ice through grounding-line retreat and increased discharge (Fig. 2a). A similar adjustment occurs in the coupled simulations: Antarctic melt rates decrease as subsurface shelf temperatures stabilize under constant CO_2 forcing (Figs. 4 and 5). This behaviour explains the lower freshwater flux in Period B than in Period A despite persistently elevated subsurface temperatures and highlights the importance of delayed ice-sheet responses for long-term climate-ice-sheet feedbacks.

Additional uncertainty arises from the parameterization of basal melting. In AIME, basal-melt forcing is computed from subsurface ocean temperatures using a quadratic thermal relation with regionally constant melt sensitivities derived from the LADDIE basal-melt model (Lambert et al., 2023). These sensitivities were calibrated for thermal forcing up to approximately 2°C, whereas simulated subsurface shelf temperatures exceed this range under abrupt-4$\times CO_2$ forcing (Fig. 5). Moreover,

https://doi.org/10.5194/egusphere-2026-4584
Preprint. Discussion started: 14 August 2026

previous studies have shown that melt sensitivity depends on both thermal forcing and cavity circulation. For example, Yung et al. (2025) demonstrated that stratification feedbacks can suppress basal melting more strongly under warm-cavity conditions than under cold-cavity conditions. The relationship between thermal forcing and basal melt may therefore evolve as ice shelves transition between different ocean and circulation regimes.

The total freshwater forcing produced by EC-Earth3-AIME in standalone mode is comparable to the ISMIP6 MeanAnt forcing (Fig. 2b), suggesting that the simulated climate response is representative of scenarios with a similar magnitude of Antarctic freshwater input. Nevertheless, considerable uncertainty remains in the magnitude and timing of the simulated response. Basal-melt sensitivities vary substantially among melt models and are further modified by changes in ice-shelf geometry. As ice shelves thin, their bases may be lifted away from relatively warm waters, reducing their sensitivity to temperatures at intermediate depths of 200–700 m (Lambert and Burgard, 2025). The ice-sheet model used to derive the LRFs also affects the magnitude and timing of freshwater release, while the climate model determines the oceanic forcing that drives basal melt (van der Linden et al., 2023). Our findings should therefore be interpreted in the context of a single climate model, a single ice-sheet model, and a single basal-melt formulation.

The representation of freshwater delivery also remains idealized. The spatial distribution and partitioning of freshwater between iceberg melt and basal melting are based on present-day observational constraints, although both are likely to evolve under strong future warming (Coulon et al., 2024). Iceberg meltwater is distributed uniformly within each ocean sector, whereas observations indicate a substantially more heterogeneous distribution (Tournadre et al., 2016). Incorporating Lagrangian iceberg models would improve the representation of iceberg drift and melt and their effects on stratification, sea ice, and regional circulation (Martin and Adcroft, 2010; Marsh et al., 2015; Zhang et al., 2025). Similarly, basal meltwater is introduced uniformly over a prescribed depth range of 200-700 m, despite considerable three-dimensional variability in the location of meltwater release (Adusumilli et al., 2020). These limitations are compounded by the 1° horizontal resolution of the ocean model, which restricts the representation of mesoscale processes that redistribute freshwater and heat across the continental shelf. Ocean configurations that explicitly resolve ice-shelf cavities, including recent developments in NEMO (Mathiot et al., 2017), provide a promising pathway toward more realistic ocean-ice coupling in future EC-Earth simulations.

Despite these limitations, our results provide robust evidence that the strength and sign of Antarctic freshwater feedbacks evolve over time. We diagnose a positive feedback of approximately +15% during the initial adjustment phase and a negative feedback of about –26% as the climate system approaches equilibrium, with transient peak values approaching +75%. This peak is comparable to the multi-model mean feedback strength of approximately +80% reported by Lambert et al. (2025). However, whereas previous studies have largely emphasized the positive feedback associated with meltwater-induced stratification, our coupled framework shows that this response progressively weakens and ultimately reverses. The reversal occurs because freshwater-induced reductions in ocean heat uptake and global warming increasingly outweigh the local enhancement of subsurface heat retention. These findings demonstrate the importance of representing coupled interactions among Antarctic melt, the Southern Ocean, and the atmosphere when assessing Antarctica's long-term influence on the climate system.

https://doi.org/10.5194/egusphere-2026-4584
Preprint. Discussion started: 14 August 2026

5 Conclusions

In this study, we integrated the Antarctic Ice Melt Emulator (AIME) into the global climate model EC-Earth3 to investigate interactions between Antarctic freshwater release, the Southern Ocean, and the global climate system. Our results reveal competing feedbacks that operate on different timescales and together regulate the long-term response of Antarctic ice-sheet melt and climate.

Freshwater release from the Antarctic Ice Sheet initially enhances subsurface warming of Antarctic shelf waters by increasing upper-ocean stratification and modifying shelf circulation. Stronger stratification suppresses vertical heat exchange, promoting subsurface heat retention and increasing the availability of ocean heat for ice-shelf melting. This response constitutes a positive feedback, as enhanced ice-shelf melting generates additional freshwater input to the Southern Ocean.

As the climate system evolves toward equilibrium, however, the influence of global climate feedbacks becomes increasingly important. Freshwater-induced reductions in surface warming reduce sea-ice loss, decrease ocean heat uptake, and lower the amount of heat stored within the climate system. As a result, less heat becomes available to warm the Southern Ocean and Antarctic continental shelf. The long-term response is therefore characterized by cooler subsurface shelf waters despite continued freshwater forcing.

Our results demonstrate that Antarctic meltwater feedbacks operate differently on transient and equilibrium timescales. During the initial adjustment phase, ocean-driven feedbacks associated with enhanced stratification and altered circulation promote subsurface warming and increased ice-shelf melt. As the climate system approaches equilibrium, reductions in ocean heat uptake and global warming increasingly outweigh these local positive feedbacks. The net effect is a transition from enhanced subsurface warming to relative subsurface cooling of Antarctic shelf waters. This competition between ocean-driven positive feedbacks and atmosphere-driven negative feedbacks has also been identified by Schloesser et al. (2019) and Li et al. (2024), although our results demonstrate how this competition evolves dynamically within a fully coupled climate-ice-sheet framework. These findings highlight the importance of distinguishing between transient and equilibrium responses when assessing Antarctic meltwater-climate interactions.

These findings reinforce the emerging view that Antarctic freshwater input exerts a first-order influence on global climate evolution through its impact on ocean heat uptake and the global energy balance. Although the magnitude of freshwater forcing in our experiments exceeds present-day and near-term projections, the mechanisms identified here are likely to remain relevant under future climate change. Representing Antarctic freshwater fluxes interactively in Earth System Models is therefore essential for improving projections of Antarctic ice-sheet evolution, Southern Ocean change, and long-term climate response.

Code and data availability.

- AIME code: https://github.com/evevadeli/ece-interactive-fwf
- Region definitions of the five LARMIP regions in Antarctica: https://www.pik-potsdam.de/en/institute/departments/earth-system-analysis/models/larmip/larmip-regions

https://doi.org/10.5194/egusphere-2026-4584
Preprint. Discussion started: 14 August 2026

- Calving and basal melt masks corresponding with the five LARMIP regions: https://github.com/erwinlambert/feedback/blob/main/data/inputfiles/runoff_maps.nc
- Total freshwater flux linear response functions: https://github.com/dlebars/LARMIPmass

https://doi.org/10.5194/egusphere-2026-4584
Preprint. Discussion started: 14 August 2026

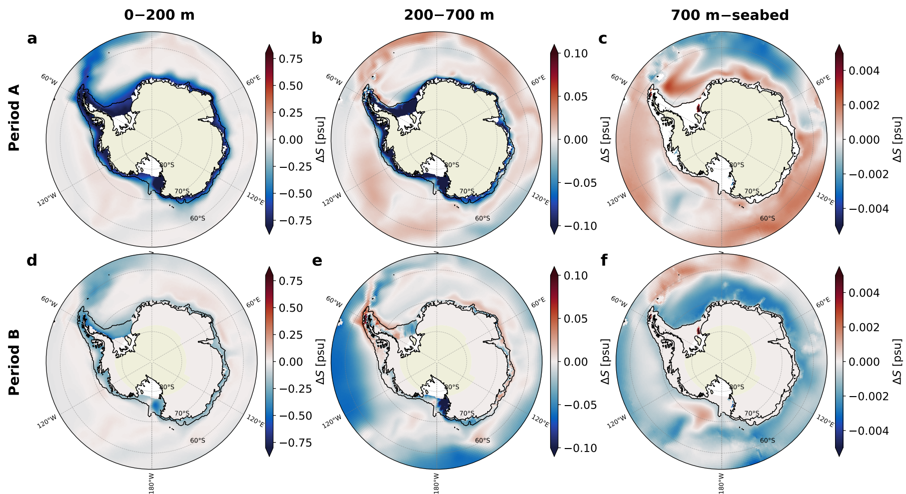

Figure A1. Depth-dependent ocean salinity anomalies under abrupt-4$\times CO_2$ forcing. Shown are salinity differences between the EC-Earth3 simulation coupled to the Antarctic Ice Melt Emulator (AIME-ON) and the EC-Earth3 CMIP6 configuration without interactive Antarctic meltwater feedbacks (NO-AIME), averaged over Period A (top row) and Period B (bottom row). Results are shown for three depth ranges: 0–200 m, 200–700 m, and 700 m to the seabed. The black contour line marks the continental shelf break, defined by the 1000 m isobath. Note that colour scales differ between columns to highlight the spatial structure of the response.

https://doi.org/10.5194/egusphere-2026-4584
Preprint. Discussion started: 14 August 2026

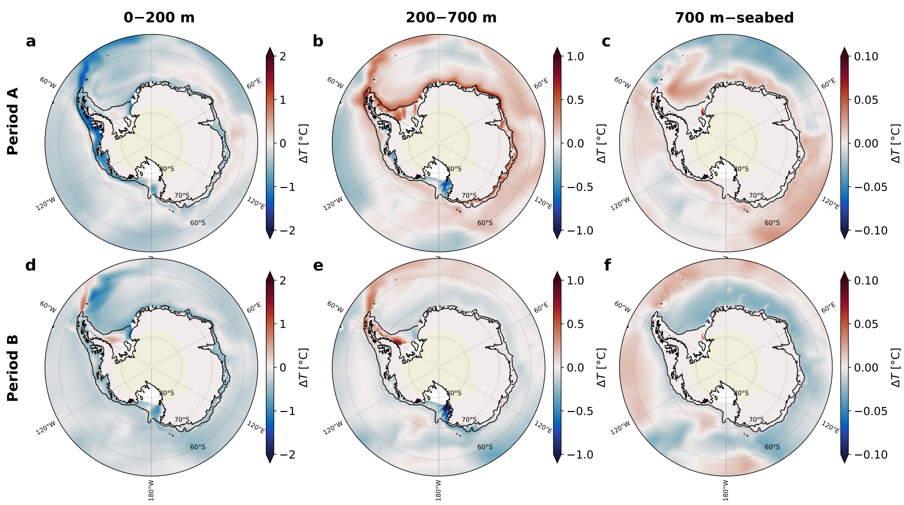

Figure A2. Depth-dependent ocean temperature anomalies under abrupt-4$\times CO_2$ forcing. Shown are temperautre differences between the EC-Earth3 simulation coupled to the Antarctic Ice Melt Emulator (AIME-ON) and the EC-Earth3 CMIP6 configuration without interactive Antarctic meltwater feedbacks (NO-AIME), averaged over Period A (top row) and Period B (bottom row). Results are shown for three depth ranges: 0–200 m, 200–700 m, and 700 m to the seabed. The black contour line marks the continental shelf break, defined by the 1000 m isobath. Note that colour scales differ between columns to highlight the spatial structure of the response.

https://doi.org/10.5194/egusphere-2026-4584
Preprint. Discussion started: 14 August 2026

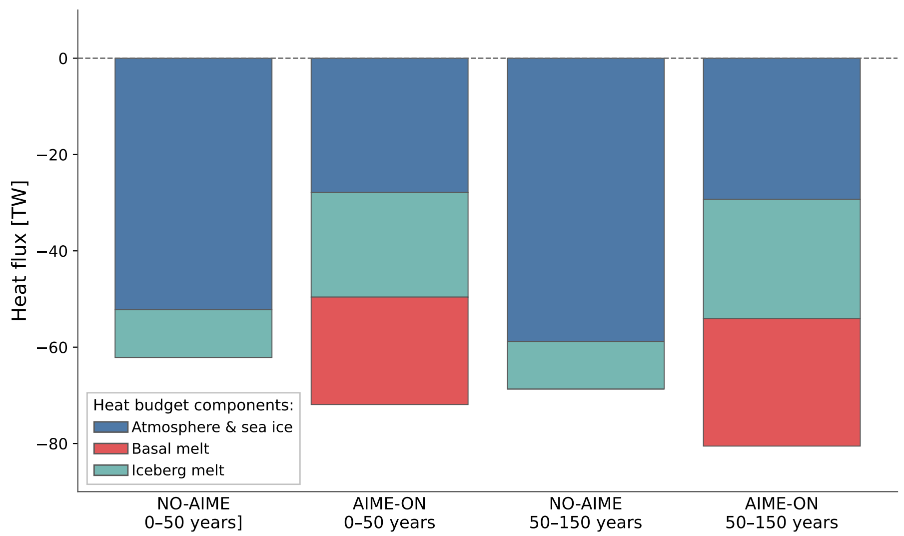

Figure A3. Shelf-integrated heat-budget components (TW) for the Antarctic continental shelf during the first 50 years (0-50 years) and the subsequent 100 years (50-150 years) in the simulations without AIME (NO-AIME) and with AIME (AIME-ON). Negative values (below the dashed horizontal line) represent heat loss from the shelf ocean through atmosphere-sea ice interactions, ice-shelf basal melt, and iceberg melt.

https://doi.org/10.5194/egusphere-2026-4584
Preprint. Discussion started: 14 August 2026

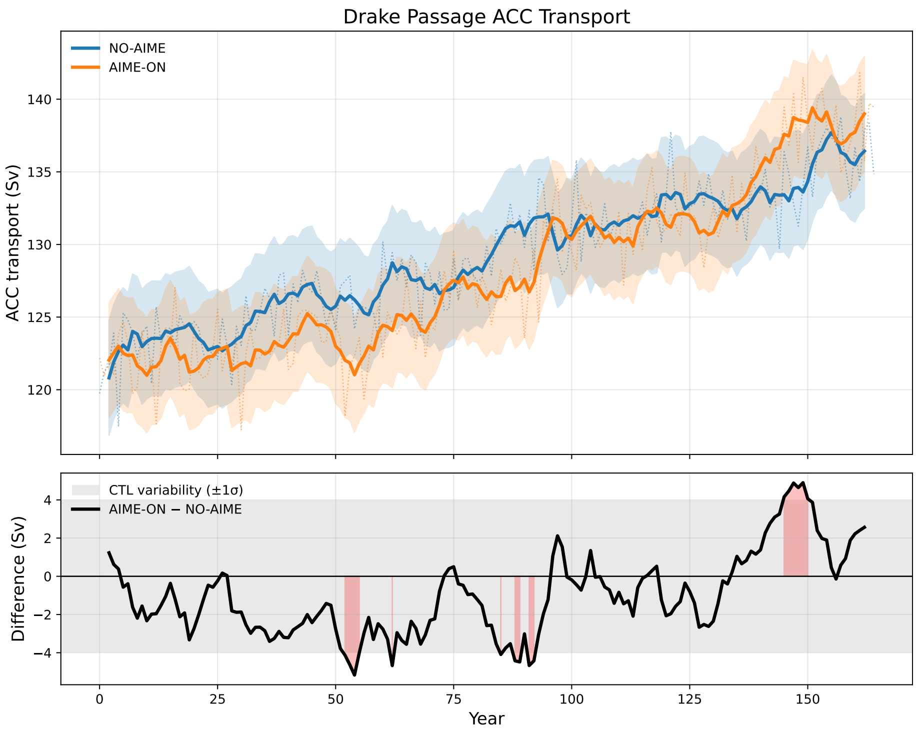

Figure A4. Drake Passage Antarctic Circumpolar Current (ACC) transport in the NO-AIME and AIME-ON experiments. Thin dotted lines show annual values, while thick solid lines show 5-year running means. Shaded envelopes around the solid lines indicate the $\pm 1\sigma$ range of 5-year mean ACC transport estimated from the 500-year CTL simulation, representing the expected internal variability. The lower panel shows the difference (AIME-ON - NO-AIME), with the grey band denoting the $\pm 1\sigma$ range of 5-year mean variability in the CTL simulation. Periods where the difference lies outside the grey band are highlighted in red, indicating that the AIME-induced response exceeds the typical magnitude of internal climate variability.

https://doi.org/10.5194/egusphere-2026-4584
Preprint. Discussion started: 14 August 2026

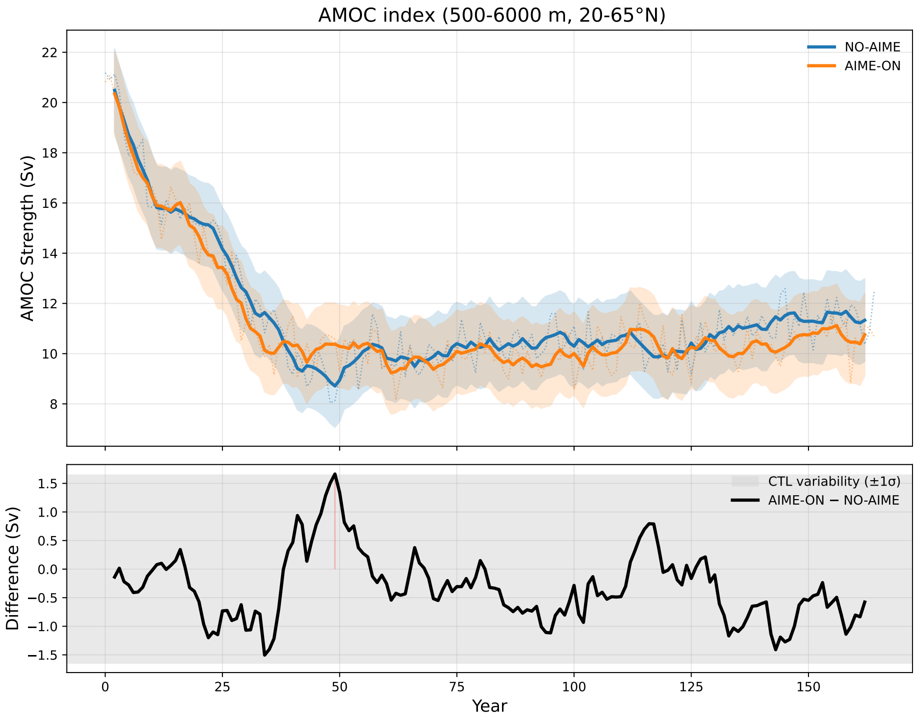

Figure A5. Atlantic Meridional Overturning Circulation (AMOC) strength in the NO-AIME and AIME-ON experiments. The AMOC index is defined as the annual maximum of the Atlantic meridional overturning streamfunction within 20-65°N and 500-6000 m depth. Thin dotted lines show annual values, while thick solid lines show 5-year running means. Shaded envelopes around the solid lines indicate the $\pm 1\sigma$ range of 5-year mean AMOC strength estimated from the 500-year CTL simulation, representing the characteristic magnitude of internal variability. The lower panel shows the difference (AIME-ON - NO-AIME), with the grey band denoting the $\pm 1\sigma$ range of 5-year mean variability in the CTL simulation. Periods where the difference lies outside the grey band are highlighted in red, indicating that the AIME-induced response exceeds the typical magnitude of internal climate variability.

https://doi.org/10.5194/egusphere-2026-4584
Preprint. Discussion started: 14 August 2026

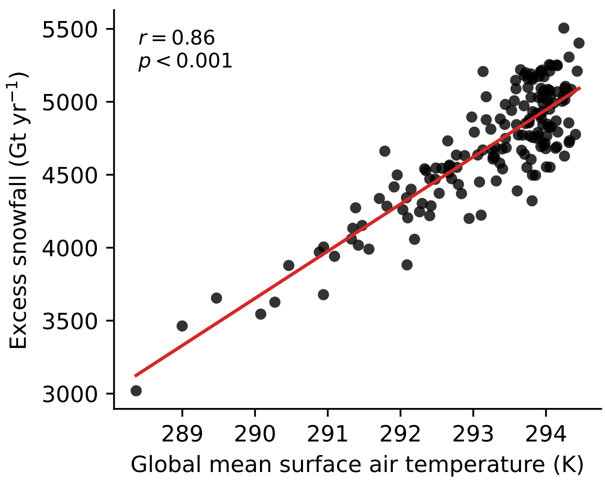

Figure A6. Relationship between global mean surface air temperature and excess snowfall in NO-AIME. Each point represents one year. The red line shows the least-squares linear regression. The Pearson correlation coefficient (r) and corresponding p-value for the regression are reported in the panel.

Author contributions. ECvdL, DLeB and SD developed the idea for this study. ECvdL, KW, and AJ developed the model code for AIME. ECvdL performed the simulations and analyses and wrote the manuscript with feedback from all co-authors.

Competing interests. The authors declare that no competing interests are present.

Acknowledgements. We thank Philippe Le Sager for his support in setting up the modelling framework. We are grateful to Anders Levermann for providing the ice mass linear response functions from the modelling groups participating in LARMIP-2. The study is financed by the Sea Level Rise Knowledge Programme of the Ministry of Infrastructure and Water Management of the Netherlands.

https://doi.org/10.5194/egusphere-2026-4584
Preprint. Discussion started: 14 August 2026

References

Adusumilli, S., Fricker, H. A., Medley, B., Padman, L., and Siegfried, M. R.: Interannual variations in meltwater input to the Southern Ocean from Antarctic ice shelves, Nat. Geosci., 13, 616–620, https://doi.org/10.1038/s41561-020-0616-z, 2020.

Basinski-Ferris, R., Zanna, L., and Eisenman, I.: Controls on the ocean response to idealized Antarctic meltwater input, https://doi.org/10.48550/arXiv.2509.19730, arXiv:2509.19730 [physics] version: 1, 2025.

Beadling, R. L., Russell, J. L., Stouffer, R. J., Mazloff, M., Talley, L. D., Goodman, P. J., Sallée, J. B., Hewitt, H. T., Hyder, P., and Pandde, A.: Representation of Southern Ocean Properties across Coupled Model Intercomparison Project Generations: CMIP3 to CMIP6, Journal of Climate, 33, 6555–6581, https://doi.org/10.1175/JCLI-D-19-0970.1, 2020.

Beadling, R. L., Krasting, J. P., Griffies, S. M., Hurlin, W. J., Bronselaer, B., Russell, J. L., MacGilchrist, G. A., Tesdal, J.-E., and Winton, M.: Importance of the Antarctic Slope Current in the Southern Ocean Response to Ice Sheet Melt and Wind Stress Change, Journal of Geophysical Research: Oceans, 127, e2021JC017 608, https://doi.org/10.1029/2021JC017608, _eprint: https://onlinelibrary.wiley.com/doi/pdf/10.1029/2021JC017608, 2022.

Bintanja, R., van Oldenborgh, G. J., Drijfhout, S. S., Wouters, B., and Katsman, C. A.: Important role for ocean warming and increased ice-shelf melt in Antarctic sea-ice expansion, Nature Geosci, 6, 376–379, https://doi.org/10.1038/ngeo1767, 2013.

Bronselaer, B., Winton, M., Griffies, S. M., Hurlin, W. J., Rodgers, K. B., Sergienko, O. V., Stouffer, R. J., and Russell, J. L.: Change in future climate due to Antarctic meltwater, Nature, 564, 53–58, https://doi.org/10.1038/s41586-018-0712-z, number: 7734, 2018.

Burgard, C., Jourdain, N. C., Mosbeux, C., Caillet, J., Mathiot, P., and Kittel, C.: Ocean warming threatens the viability of 60% of Antarctic ice shelves, Nature, pp. 1–7, https://doi.org/10.1038/s41586-025-09657-w, 2025.

Coulon, V., De Rydt, J., Gregov, T., Qin, Q., and Pattyn, F.: Future Freshwater Fluxes From the Antarctic Ice Sheet, Geophysical Research Letters, 51, e2024GL111 250, https://doi.org/10.1029/2024GL111250, _eprint: https://agupubs.onlinelibrary.wiley.com/doi/pdf/10.1029/2024GL111250, 2024.

Depoorter, M. A., Bamber, J. L., Griggs, J. A., Lenaerts, J. T. M., Ligtenberg, S. R. M., van den Broeke, M. R., and Moholdt, G.: Calving fluxes and basal melt rates of Antarctic ice shelves, Nature, 502, 89–92, https://doi.org/10.1038/nature12567, 2013.

Döscher, R., Acosta, M., Alessandri, A., Anthoni, P., Arsouze, T., Bergman, T., Bernardello, R., Boussetta, S., Caron, L.-P., Carver, G., Castrillo, M., Catalano, F., Cvijanovic, I., Davini, P., Dekker, E., Doblas-Reyes, F. J., Docquier, D., Echevarria, P., Fladrich, U., Fuentes-Franco, R., Gröger, M., v. Hardenberg, J., Hieronymus, J., Karami, M. P., Keskinen, J.-P., Koenigk, T., Makkonen, R., Massonnet, F., Ménégoz, M., Miller, P. A., Moreno-Chamarro, E., Nieradzik, L., van Noije, T., Nolan, P., O'Donnell, D., Ollinaho, P., van den Oord, G., Ortega, P., Prims, O. T., Ramos, A., Reerink, T., Rousset, C., Ruprich-Robert, Y., Le Sager, P., Schmith, T., Schrödner, R., Serva, F., Sicardi, V., Sloth Madsen, M., Smith, B., Tian, T., Tourigny, E., Uotila, P., Vancoppenolle, M., Wang, S., Wårlind, D., Willén, U., Wyser, K., Yang, S., Yepes-Arbós, X., and Zhang, Q.: The EC-Earth3 Earth system model for the Coupled Model Intercomparison Project 6, Geoscientific Model Development, 15, 2973–3020, https://doi.org/10.5194/gmd-15-2973-2022, 2022.

Fyke, J., Sergienko, O., Löfverström, M., Price, S., and Lenaerts, J. T. M.: An Overview of Interactions and Feedbacks Between Ice Sheets and the Earth System, Reviews of Geophysics, 56, 361–408, https://doi.org/10.1029/2018RG000600, _eprint: https://onlinelibrary.wiley.com/doi/pdf/10.1029/2018RG000600, 2018.

Gierz, P., Ackermann, L., Rodehacke, C. B., Krebs-Kanzow, U., Stepanek, C., Barbi, D., and Lohmann, G.: Simulating interactive ice sheets in the multi-resolution AWI-ESM 1.2: A case study using SCOPE 1.0, Geoscientific Model Development Discussions, pp. 1–32, https://doi.org/10.5194/gmd-2020-159, 2020.

https://doi.org/10.5194/egusphere-2026-4584
Preprint. Discussion started: 14 August 2026

Golledge, N. R., Keller, E. D., Gomez, N., Naughten, K. A., Bernales, J., Trusel, L. D., and Edwards, T. L.: Global environmental consequences of twenty-first-century ice-sheet melt, Nature, 566, 65–72, https://doi.org/10.1038/s41586-019-0889-9, number: 7742, 2019.

Gorte, T., Lovenduski, N. S., Nissen, C., and Lenaerts, J. T. M.: Antarctic Ice Sheet Freshwater Discharge Drives Substantial Southern Ocean Changes Over the 21st Century, Geophysical Research Letters, 50, e2023GL104 949, https://doi.org/10.1029/2023GL104949, _eprint: https://agupubs.onlinelibrary.wiley.com/doi/pdf/10.1029/2023GL104949, 2023.

Gudmundsson, G. H.: Ice-shelf buttressing and the stability of marine ice sheets, The Cryosphere, 7, 647–655, https://doi.org/10.5194/tc-7-647-2013, 2013.

Hill, E. A., Gudmundsson, G. H., and Chandler, D. M.: Ocean warming as a trigger for irreversible retreat of the Antarctic ice sheet, Nat. Clim. Chang., 14, 1165–1171, https://doi.org/10.1038/s41558-024-02134-8, 2024.

Holland, D. M., Nicholls, K. W., and Basinski, A.: The Southern Ocean and its interaction with the Antarctic Ice Sheet, Science, 367, 1326–1330, https://doi.org/10.1126/science.aaz5491, 2020.

Jenkins, A., Dutrieux, P., Jacobs, S. S., McPhail, S. D., Perrett, J. R., Webb, A. T., and White, D.: Observations beneath Pine Island Glacier in West Antarctica and implications for its retreat, Nature Geosci, 3, 468–472, https://doi.org/10.1038/ngeo890, 2010.

Lambert, E. and Burgard, C.: Brief communication: Sensitivity of Antarctic ice shelf melting to ocean warming across basal melt models, The Cryosphere, 19, 2495–2505, https://doi.org/10.5194/tc-19-2495-2025, 2025.

Lambert, E., Jüling, A., van de Wal, R. S. W., and Holland, P. R.: Modelling Antarctic ice shelf basal melt patterns using the one-layer Antarctic model for dynamical downscaling of ice–ocean exchanges (LADDIE v1.0), The Cryosphere, 17, 3203–3228, https://doi.org/10.5194/tc-17-3203-2023, 2023.

Lambert, E., Le Bars, D., van der Linden, E., Jüling, A., and Drijfhout, S.: Quantifying the feedback between Antarctic meltwater release and subsurface Southern Ocean warming, Earth System Dynamics, 16, 1303–1323, https://doi.org/10.5194/esd-16-1303-2025, 2025.

Levermann, A., Winkelmann, R., Albrecht, T., Goelzer, H., Golledge, N. R., Greve, R., Huybrechts, P., Jordan, J., Leguy, G., Martin, D., Morlighem, M., Pattyn, F., Pollard, D., Quiquet, A., Rodehacke, C., Seroussi, H., Sutter, J., Zhang, T., Van Breedam, J., Calov, R., DeConto, R., Dumas, C., Garbe, J., Gudmundsson, G. H., Hoffman, M. J., Humbert, A., Kleiner, T., Lipscomb, W. H., Meinshausen, M., Ng, E., Nowicki, S. M. J., Perego, M., Price, S. F., Saito, F., Schlegel, N.-J., Sun, S., and van de Wal, R. S. W.: Projecting Antarctica's contribution to future sea level rise from basal ice shelf melt using linear response functions of 16 ice sheet models (LARMIP-2), Earth System Dynamics, 11, 35–76, https://doi.org/10.5194/esd-11-35-2020, 2020.

Li, D.: Physical processes and feedbacks obscuring the future of the Antarctic Ice Sheet, Geosystems and Geoenvironment, 1, 100 084, https://doi.org/10.1016/j.geogeo.2022.100084, 2022.

Li, D., DeConto, R. M., Pollard, D., and Hu, Y.: Competing climate feedbacks of ice sheet freshwater discharge in a warming world, Nat Commun, 15, 5178, https://doi.org/10.1038/s41467-024-49604-3, 2024.

Mackie, S., Smith, I. J., Ridley, J. K., Stevens, D. P., and Langhorne, P. J.: Climate Response to Increasing Antarctic Iceberg and Ice Shelf Melt, https://doi.org/10.1175/JCLI-D-19-0881.1, 2020a.

Mackie, S., Smith, I. J., Stevens, D. P., Ridley, J. K., and Langhorne, P. J.: Interactions between Increasing CO2 and Antarctic Melt Rates, https://doi.org/10.1175/JCLI-D-19-0882.1, 2020b.

Marsh, R., Ivchenko, V. O., Skliris, N., Alderson, S., Bigg, G. R., Madec, G., Blaker, A. T., Aksenov, Y., Sinha, B., Coward, A. C., Le Sommer, J., Merino, N., and Zalesny, V. B.: NEMO–ICB (v1.0): interactive icebergs in the NEMO ocean model globally configured at eddy-permitting resolution, Geoscientific Model Development, 8, 1547–1562, https://doi.org/10.5194/gmd-8-1547-2015, 2015.

https://doi.org/10.5194/egusphere-2026-4584
Preprint. Discussion started: 14 August 2026

Martin, T. and Adcroft, A.: Parameterizing the fresh-water flux from land ice to ocean with interactive icebergs in a coupled climate model, Ocean Modelling, 34, 111–124, https://doi.org/10.1016/j.ocemod.2010.05.001, 2010.

Mathiot, P., Jenkins, A., Harris, C., and Madec, G.: Explicit representation and parametrised impacts of under ice shelf seas in the z^* coordinate ocean model NEMO 3.6, Geoscientific Model Development, 10, 2849–2874, https://doi.org/10.5194/gmd-10-2849-2017, 2017.

Mistry, A., Lunt, D., and Ren, X.: Global climate system response to SOFIA Antarctic meltwater in HadCM3-M2.1, The Cryosphere, 19, 6989–7012, https://doi.org/10.5194/tc-19-6989-2025, 2025.

Moon, J.-Y., An, S.-I., Mandal, G., Song, H., Yang, Y.-M., and Park, S.-E.: Antarctic meltwater spread pattern and its duration modulate abyssal circulation, Commun Earth Environ, 6, 586, https://doi.org/10.1038/s43247-025-02589-3, 2025.

Muilwijk, M., Hattermann, T., Beadling, R. L., Swart, N. C., Nummelin, A., Guo, C., Chandler, D. M., Langebroek, P., Zhou, S., Dutrieux, P., Chen, J.-J., Danek, C., England, M. H., Griffies, S. M., Haumann, F. A., Jüling, A., Jouet, O., Li, Q., Martin, T., Marshall, J., Pauling, A. G., Purich, A., Song, Z., Smith, I. J., Thomas, M., Trombini, I., van der Linden, E., and Xu, X.: Large Regional Differences in Antarctic Ice Shelf Mass Loss from Southern Ocean Warming and Meltwater Feedbacks, EGUsphere, pp. 1–39, https://doi.org/10.5194/egusphere-2025-3747, 2025.

Nowicki, S. M. J., Payne, A., Larour, E., Seroussi, H., Goelzer, H., Lipscomb, W., Gregory, J., Abe-Ouchi, A., and Shepherd, A.: Ice Sheet Model Intercomparison Project (ISMIP6) contribution to CMIP6, Geoscientific Model Development, 9, 4521–4545, https://doi.org/10.5194/gmd-9-4521-2016, 2016.

Ong, E. Q. Y., England, M. H., Doddridge, E., and Constantinou, N. C.: Transient Antarctic Slope Current Response to Climate Change Including Meltwater, Geophysical Research Letters, 52, e2024GL113 983, https://doi.org/10.1029/2024GL113983, _eprint: https://onlinelibrary.wiley.com/doi/pdf/10.1029/2024GL113983, 2025.

Paolo, F. S., Fricker, H. A., and Padman, L.: Volume loss from Antarctic ice shelves is accelerating, Science, 348, 327–331, https://doi.org/10.1126/science.aaa0940, 2015.

Park, J.-Y., Schloesser, F., Timmermann, A., Choudhury, D., Lee, J.-Y., and Nellikkattil, A. B.: Future sea-level projections with a coupled atmosphere-ocean-ice-sheet model, Nat Commun, 14, 636, https://doi.org/10.1038/s41467-023-36051-9, 2023.

Park, W. and Latif, M.: Ensemble global warming simulations with idealized Antarctic meltwater input, Clim Dyn, 52, 3223–3239, https://doi.org/10.1007/s00382-018-4319-8, 2019.

Pattyn, F.: Sea-level response to melting of Antarctic ice shelves on multi-centennial timescales with the fast Elementary Thermomechanical Ice Sheet model (f.ETISh v1.0), The Cryosphere, 11, 1851–1878, https://doi.org/10.5194/tc-11-1851-2017, 2017.

Pauling, A. G., Bitz, C. M., Smith, I. J., and Langhorne, P. J.: The Response of the Southern Ocean and Antarctic Sea Ice to Freshwater from Ice Shelves in an Earth System Model, Journal of Climate, 29, 1655–1672, https://doi.org/10.1175/JCLI-D-15-0501.1, 2016.

Pauling, A. G., Smith, I. J., Martin, T., Ridley, J. K., Stevens, D. P., Thomas, M., Beadling, R. L., Danek, C., Hattermann, T., Li, Q., Marshall, J., Muilwijk, M., Purich, A., and Swart, N. C.: Antarctic sea ice response to meltwater due to Antarctic ice sheet mass loss in a multi-model ensemble, EGUsphere, pp. 1–29, https://doi.org/10.5194/egusphere-2026-658, 2026.

Pritchard, H. D., Ligtenberg, S. R. M., Fricker, H. A., Vaughan, D. G., van den Broeke, M. R., and Padman, L.: Antarctic ice-sheet loss driven by basal melting of ice shelves, Nature, 484, 502–505, https://doi.org/10.1038/nature10968, 2012.

Purich, A. and England, M. H.: Projected Impacts of Antarctic Meltwater Anomalies over the Twenty-First Century, Journal of Climate, 36, 2703–2719, https://doi.org/10.1175/JCLI-D-22-0457.1, 2023.

Rignot, E., Jacobs, S., Mouginot, J., and Scheuchl, B.: Ice-Shelf Melting Around Antarctica, Science, 341, 266–270, https://doi.org/10.1126/science.1235798, 2013.

Rignot, E., Mouginot, J., Scheuchl, B., van den Broeke, M., van Wessem, M. J., and Morlighem, M.: Four decades of Antarctic Ice Sheet mass balance from 1979–2017, Proceedings of the National Academy of Sciences, 116, 1095–1103, https://doi.org/10.1073/pnas.1812883116, 2019.

Rye, C. D., Marshall, J., Kelley, M., Russell, G., Nazarenko, L. S., Kostov, Y., Schmidt, G. A., and Hansen, J.: Antarctic Glacial Melt as a Driver of Recent Southern Ocean Climate Trends, Geophysical Research Letters, 47, e2019GL086 892, https://doi.org/10.1029/2019GL086892, _eprint: https://onlinelibrary.wiley.com/doi/pdf/10.1029/2019GL086892, 2020.

Sadai, S., Condron, A., DeConto, R., and Pollard, D.: Future climate response to Antarctic Ice Sheet melt caused by anthropogenic warming, Science Advances, 6, eaaz1169, https://doi.org/10.1126/sciadv.aaz1169, 2020.

Sadai, S., Karmalkar, A. V., Pollard, D., Dong, Y., Lucas, E., Gomez, N., DeConto, R., and Condron, A.: Antarctic meltwater alters future projections of climate and sea level, Nat Commun, 16, 9271, https://doi.org/10.1038/s41467-025-64438-3, 2025.

Schloesser, F., Friedrich, T., Timmermann, A., DeConto, R. M., and Pollard, D.: Antarctic iceberg impacts on future Southern Hemisphere climate, Nat. Clim. Chang., 9, 672–677, https://doi.org/10.1038/s41558-019-0546-1, number: 9, 2019.

Seroussi, H., Nowicki, S., Payne, A. J., Goelzer, H., Lipscomb, W. H., Abe-Ouchi, A., Agosta, C., Albrecht, T., Asay-Davis, X., Barthel, A., Calov, R., Cullather, R., Dumas, C., Galton-Fenzi, B. K., Gladstone, R., Golledge, N. R., Gregory, J. M., Greve, R., Hattermann, T., Hoffman, M. J., Humbert, A., Huybrechts, P., Jourdain, N. C., Kleiner, T., Larour, E., Leguy, G. R., Lowry, D. P., Little, C. M., Morlighem, M., Pattyn, F., Pelle, T., Price, S. F., Quiquet, A., Reese, R., Schlegel, N.-J., Shepherd, A., Simon, E., Smith, R. S., Straneo, F., Sun, S., Trusel, L. D., Van Breedam, J., van de Wal, R. S. W., Winkelmann, R., Zhao, C., Zhang, T., and Zwinger, T.: ISMIP6 Antarctica: a multi-model ensemble of the Antarctic ice sheet evolution over the 21st century, The Cryosphere, 14, 3033–3070, https://doi.org/10.5194/tc-14-3033-2020, 2020.

Seroussi, H., Pelle, T., Lipscomb, W. H., Abe-Ouchi, A., Albrecht, T., Alvarez-Solas, J., Asay-Davis, X., Barre, J.-B., Berends, C. J., Bernales, J., Blasco, J., Caillet, J., Chandler, D. M., Coulon, V., Cullather, R., Dumas, C., Galton-Fenzi, B. K., Garbe, J., Gillet-Chaulet, F., Gladstone, R., Goelzer, H., Golledge, N., Greve, R., Gudmundsson, G. H., Han, H. K., Hillebrand, T. R., Hoffman, M. J., Huybrechts, P., Jourdain, N. C., Klose, A. K., Langebroek, P. M., Leguy, G. R., Lowry, D. P., Mathiot, P., Montoya, M., Morlighem, M., Nowicki, S., Pattyn, F., Payne, A. J., Quiquet, A., Reese, R., Robinson, A., Saraste, L., Simon, E. G., Sun, S., Twarog, J. P., Trusel, L. D., Urruty, B., Van Breedam, J., van de Wal, R. S. W., Wang, Y., Zhao, C., and Zwinger, T.: Evolution of the Antarctic Ice Sheet Over the Next Three Centuries From an ISMIP6 Model Ensemble, Earth's Future, 12, e2024EF004 561, https://doi.org/10.1029/2024EF004561, _eprint: https://agupubs.onlinelibrary.wiley.com/doi/pdf/10.1029/2024EF004561, 2024.

Siahaan, A., Smith, R. S., Holland, P. R., Jenkins, A., Gregory, J. M., Lee, V., Mathiot, P., Payne, A. J., Ridley, J. K., and Jones, C. G.: The Antarctic contribution to 21st-century sea-level rise predicted by the UK Earth System Model with an interactive ice sheet, The Cryosphere, 16, 4053–4086, https://doi.org/10.5194/tc-16-4053-2022, 2022.

Smith, R. S., Mathiot, P., Siahaan, A., Lee, V., Cornford, S. L., Gregory, J. M., Payne, A. J., Jenkins, A., Holland, P. R., Ridley, J. K., and Jones, C. G.: Coupling the U.K. Earth System Model to Dynamic Models of the Greenland and Antarctic Ice Sheets, Journal of Advances in Modeling Earth Systems, 13, e2021MS002 520, https://doi.org/10.1029/2021MS002520, _eprint: https://onlinelibrary.wiley.com/doi/pdf/10.1029/2021MS002520, 2021.

Swart, N. C. and Fyfe, J. C.: The influence of recent Antarctic ice sheet retreat on simulated sea ice area trends, Geophysical Research Letters, 40, 4328–4332, https://doi.org/10.1002/grl.50820, _eprint: https://onlinelibrary.wiley.com/doi/pdf/10.1002/grl.50820, 2013.

Swart, N. C., Martin, T., Beadling, R., Chen, J.-J., Danek, C., England, M. H., Farneti, R., Griffies, S. M., Hattermann, T., Hauck, J., Haumann, F. A., Jüling, A., Li, Q., Marshall, J., Muilwijk, M., Pauling, A. G., Purich, A., Smith, I. J., and Thomas, M.: The Southern Ocean

https://doi.org/10.5194/egusphere-2026-4584
Preprint. Discussion started: 14 August 2026

Freshwater Input from Antarctica (SOFIA) Initiative: scientific objectives and experimental design, Geoscientific Model Development, 16, 7289–7309, https://doi.org/10.5194/gmd-16-7289-2023, 2023.

Thomas, M., Ridley, J. K., Smith, I. J., Stevens, D. P., Holland, P. R., and Mackie, S.: Future Response of Antarctic Continental Shelf Temperatures to Ice Shelf Basal Melting and Calving, Geophysical Research Letters, 50, e2022GL102 101, https://doi.org/10.1029/2022GL102101, _eprint: https://agupubs.onlinelibrary.wiley.com/doi/pdf/10.1029/2022GL102101, 2023.

Thompson, A. F., Stewart, A. L., Spence, P., and Heywood, K. J.: The Antarctic Slope Current in a Changing Climate, Reviews of Geophysics, 56, 741–770, https://doi.org/10.1029/2018RG000624, _eprint: https://onlinelibrary.wiley.com/doi/pdf/10.1029/2018RG000624, 2018.

Tournadre, J., Bouhier, N., Girard-Ardhuin, F., and Rémy, F.: Antarctic icebergs distributions 1992–2014, Journal of Geophysical Research: Oceans, 121, 327–349, https://doi.org/10.1002/2015JC011178, _eprint: https://agupubs.onlinelibrary.wiley.com/doi/pdf/10.1002/2015JC011178, 2016.

van der Linden, E. C., Le Bars, D., Lambert, E., and Drijfhout, S.: Antarctic contribution to future sea level from ice shelf basal melt as constrained by ice discharge observations, The Cryosphere, 17, 79–103, https://doi.org/10.5194/tc-17-79-2023, 2023.

Wyser, K., van Noije, T., Yang, S., von Hardenberg, J., O'Donnell, D., and Döscher, R.: On the increased climate sensitivity in the EC-Earth model from CMIP5 to CMIP6, Geoscientific Model Development, 13, 3465–3474, https://doi.org/10.5194/gmd-13-3465-2020, 2020.

Yung, C. K., Rosevear, M. G., Morrison, A. K., Hogg, A. M., and Nakayama, Y.: Stratified suppression of turbulence in an ice shelf basal melt parameterisation, The Cryosphere, 19, 5827–5861, https://doi.org/10.5194/tc-19-5827-2025, 2025.

Zehrung, A., King, A. D., Nicholls, Z., Zelinka, M. D., and Meinshausen, M.: Standardising the "Gregory method" for calculating equilibrium climate sensitivity, EGUsphere, pp. 1–26, https://doi.org/10.5194/egusphere-2025-2252, 2025.

Zhang, J., Zhang, X., King, M. A., and Lyu, K.: The response of the Southern ocean to Climatological iceberg freshwater forcing, Clim Dyn, 63, 440, https://doi.org/10.1007/s00382-025-07922-2, 2025.